KU LEUVEN

Wave Mechanics Seminar
TU Delft
May 19, 2014

The numerical solution of large scale dynamic soil–structure interaction problems

Pieter Coulier

pieter.coulier@bwk.kuleuven.be
bwk.kuleuven.be/bwm

KU Leuven, Department of Civil Engineering, Belgium

Motivation and problem outline

- Dynamic analysis of civil engineering structures:
  - buildings, bridges, nuclear power plants, . . . subjected to earthquakes

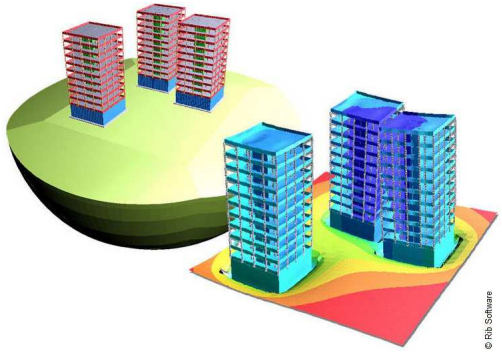

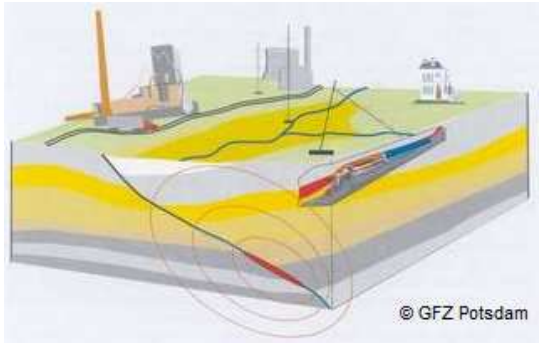

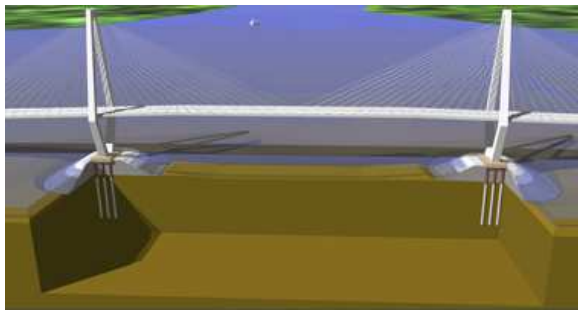

  - offshore structures exposed to wind and wave loadings

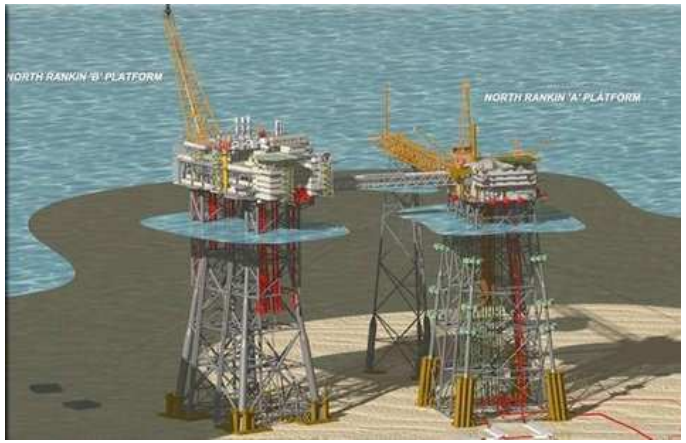

Motivation and problem outline

- Dynamic analysis of civil engineering structures:
  - blast loadings, construction activities, industrial processes, ...

  - road and railway traffic ($1 - 80\,\mathrm{Hz}$)

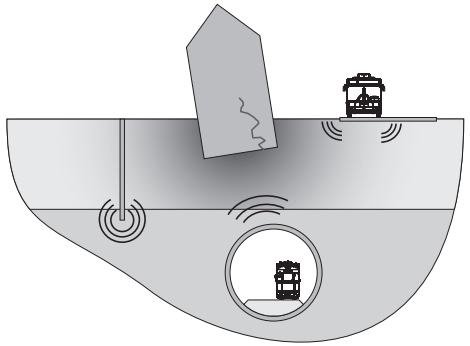

Motivation and problem outline

- Consequences of vibrations ($\sim$ amplitude, # cycles, ...):
  - Malfunctioning of sensitive equipment
  - Discomfort to people
  - Structural damage

  $\Rightarrow$ reduction of serviceability and loss of economic value

  $\Rightarrow$ considerable societal and economic importance




- Numerical models are indispensable:
  - understanding of the underlying phenomena
  - design of efficient countermeasures

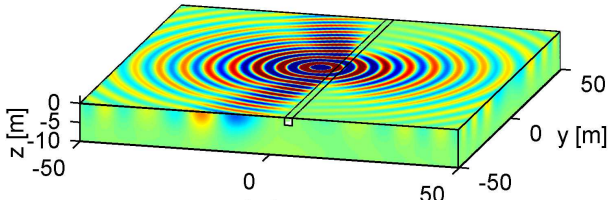

- **Dynamic soil–structure interaction** (SSI) often plays a crucial role and should be accounted for in these numerical models

Motivation and problem outline

- Accounting for dynamic SSI in numerical models is a challenging task:
  - wave propagation in the soil (semi–infinite, layered medium)
  - dynamic behaviour of the structure(s)

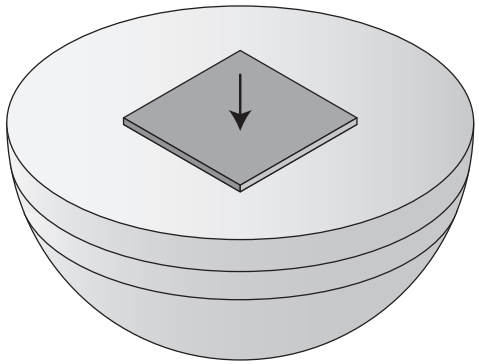

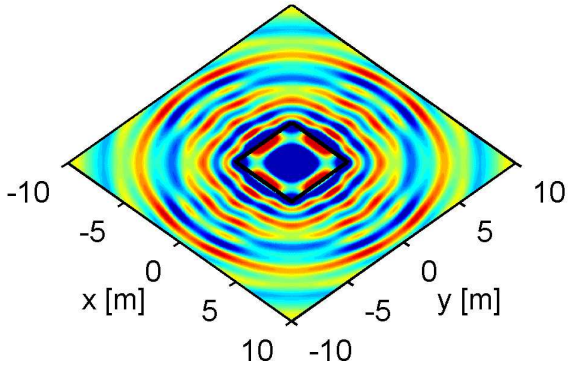

- Substantial progress has been made over the past decades:
  - Moore's law: exponential increase of computing power
  - development of a variety of numerical techniques

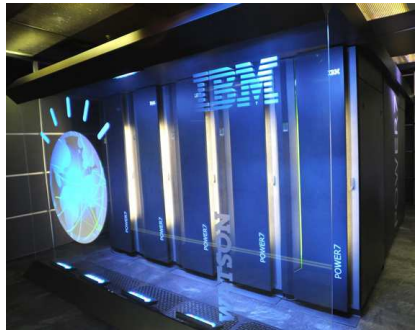

- **The numerical solution of many large scale dynamic SSI problems remains very challenging and in many cases beyond current computer capabilities**

Objectives

- The numerical solution of large 3D dynamic SSI problems remains very challenging and in many cases beyond current computer capabilities
- Fast methods for large scale dynamic SSI problems:
  - 3D BE method based on $\mathscr{H}$–matrices
  - Innovative techniques for the coupling of FE and $\mathscr{H}$-BE models
  - 2.5D FE–BE method with spatial windowing
- Applications related to the prediction of railway induced vibrations:
  - Vibration mitigation measures on the propagation path in the soil
  - Wave propagation in an urban environment
  - The influence of source–receiver interaction

Objectives

- The numerical solution of large 3D dynamic SSI problems remains very challenging and in many cases beyond current computer capabilities
- Fast methods for large scale dynamic SSI problems
  - 3D BE method based on $\mathscr{H}$–matrices
  - Innovative techniques for the coupling of FE and $\mathscr{H}$-BE models
  - 2.5D FE–BE method with spatial windowing
- Applications related to the prediction of railway induced vibrations:
  - Vibration mitigation measures on the propagation path in the soil
  - Wave propagation in an urban environment
  - The influence of source–receiver interaction

Coupled FE–BE methods for dynamic SSI problems

- Domain decomposition [Aubry et al., WAVE, 1994]:
  - Structural domain Ω_b: finite element method

$$\left[\mathbf{K}_\mathrm{b} + i\omega\mathbf{C}_\mathrm{b} - \omega^2\mathbf{M}_\mathrm{b}\right] \underline{\hat{\mathbf{u}}}_\mathrm{b}(\omega) = \underline{\hat{\mathbf{f}}}_\mathrm{b}(\omega) + \underline{\hat{\mathbf{f}}}^\mathrm{s}_\mathrm{b}(\omega)$$

  - Soil domain Ω_s: boundary element method

$$\widehat{\mathbf{U}}(\omega)\underline{\hat{\mathbf{t}}}(\omega) = \left[\widehat{\mathbf{T}}(\omega) + \mathbf{I}\right] \underline{\hat{\mathbf{u}}}(\omega)$$

- (a) Three–dimensional (3D) and (b) two–and–a–half–dimensional (2.5D) formulations

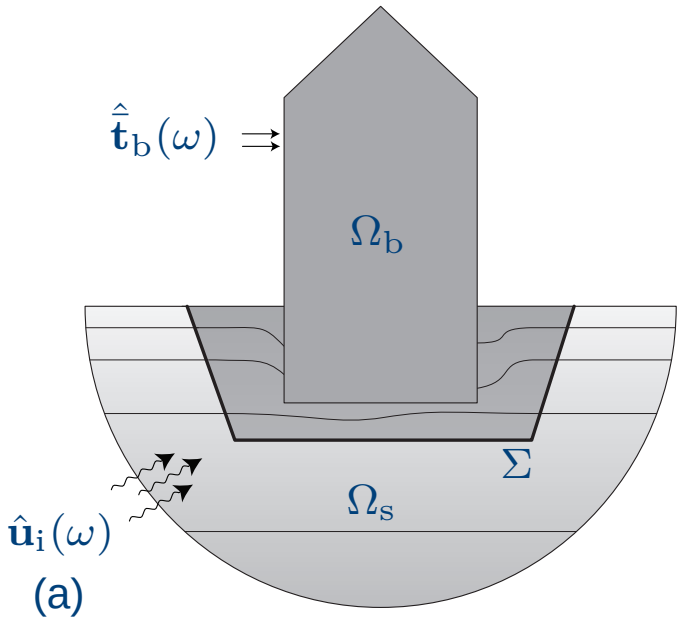

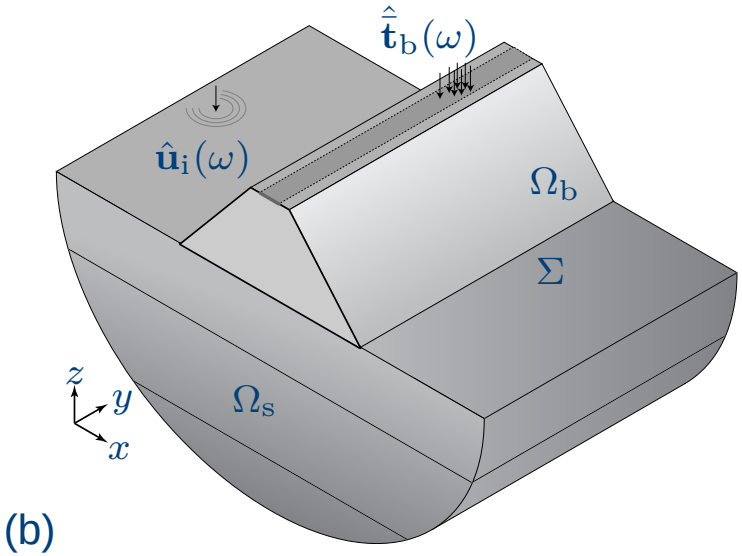

Coupled FE–BE methods for dynamic SSI problems

- Domain decomposition [Aubry et al., WAVE, 1994]:
  - Structural domain Ω_b: finite element method

$$\left[\mathbf{K}_\mathrm{b} + i\omega\mathbf{C}_\mathrm{b} - \omega^2\mathbf{M}_\mathrm{b}\right] \underline{\hat{\mathbf{u}}}_\mathrm{b}(\omega) = \underline{\hat{\mathbf{f}}}_\mathrm{b}(\omega) + \underline{\hat{\mathbf{f}}}^\mathrm{s}_\mathrm{b}(\omega)$$

  - Soil domain Ω_s: boundary element method

$$\widehat{\mathbf{U}}(\omega)\underline{\hat{\mathbf{t}}}(\omega) = \left[\widehat{\mathbf{T}}(\omega) + \mathbf{I}\right] \underline{\hat{\mathbf{u}}}(\omega)$$

- (a) Three–dimensional (3D) and (b) two–and–a–half–dimensional (2.5D) formulations

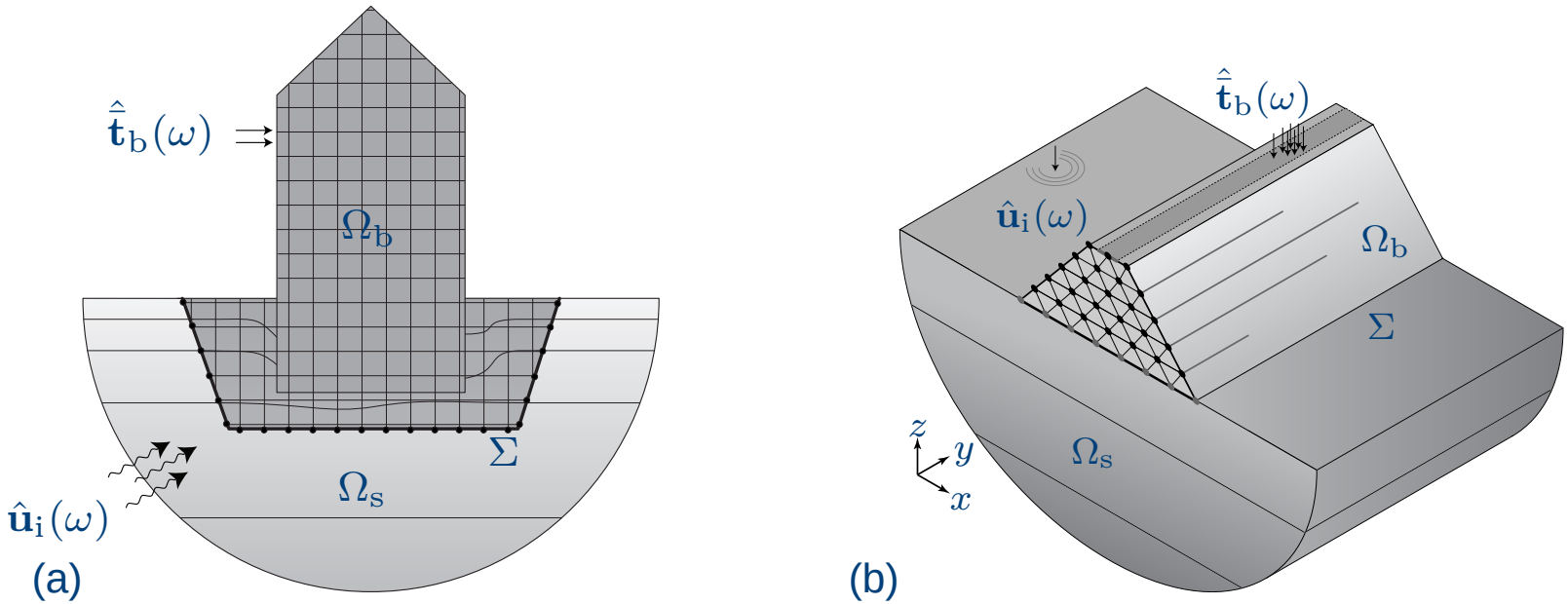

Coupled FE–BE methods for dynamic SSI problems

- Coupled FE–BE methods offer a large modelling flexibility, but at a high computational cost
- FE matrices: sparse, symmetric
- BE matrices: dense, unsymmetric

$\mathbf{K}_\mathrm{b}, \mathbf{C}_\mathrm{b}, \mathbf{M}_\mathrm{b}$

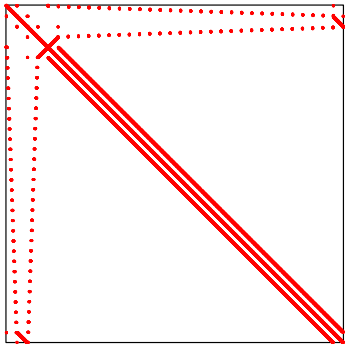

$\widehat{\mathbf{U}}(\omega), \widehat{\mathbf{T}}(\omega)$

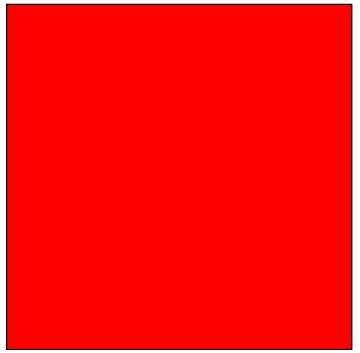

- The model size increases if:
  - the frequency range of interest increases: seismic analysis ($< 10\,\mathrm{Hz}$) vs. prediction of railway induced vibrations ($1 - 80\,\mathrm{Hz}$)
  - multiple structures are accounted for

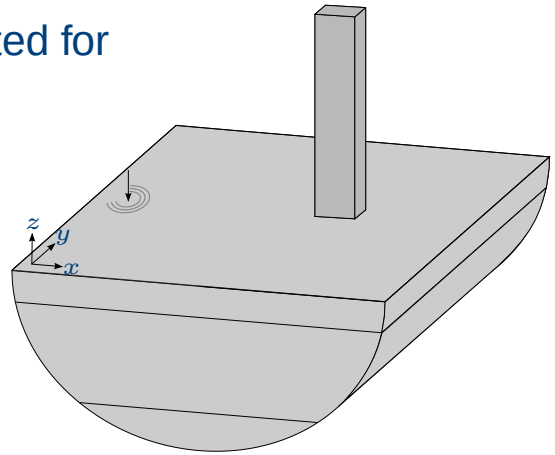

Coupled FE–BE methods for dynamic SSI problems

- Coupled FE–BE methods offer a large modelling flexibility, but at a high computational cost
- FE matrices: sparse, symmetric
- BE matrices: dense, unsymmetric

$\mathbf{K}_\mathrm{b}, \mathbf{C}_\mathrm{b}, \mathbf{M}_\mathrm{b}$

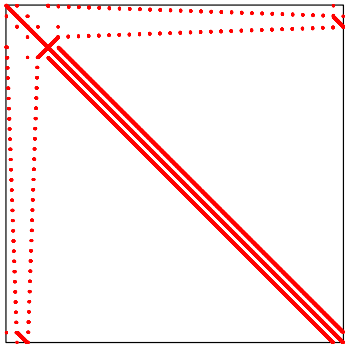

$\widehat{\mathbf{U}}(\omega), \widehat{\mathbf{T}}(\omega)$

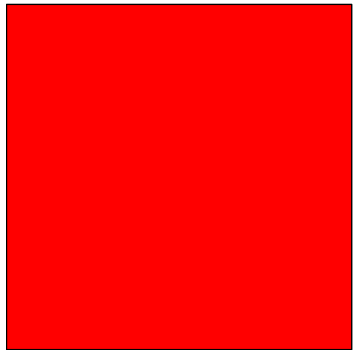

- The model size increases if:
  - the frequency range of interest increases: seismic analysis ($< 10\,\mathrm{Hz}$) vs. prediction of railway induced vibrations ($1 - 80\,\mathrm{Hz}$)
  - multiple structures are accounted for

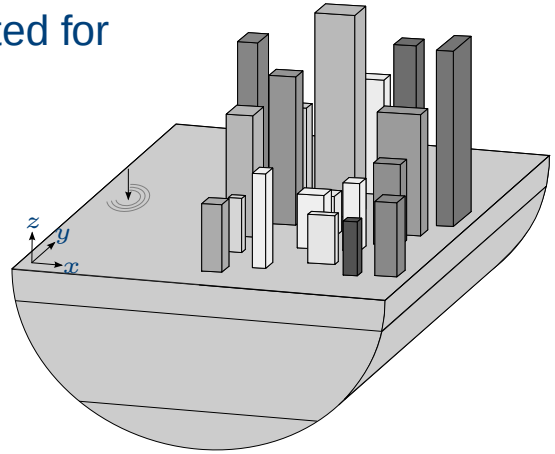

3D BE method based on $\mathscr{H}$–matrices

- Algebraic tool to approximate the BE matrices $\widehat{\mathbf{U}}(\omega)$ and $\widehat{\mathbf{T}}(\omega)$ by their hierarchical representations $\widehat{\mathbf{U}}_{\mathscr{H}}(\omega)$ and $\widehat{\mathbf{T}}_{\mathscr{H}}(\omega)$ [Hackbusch, COMPUTING, 1999]

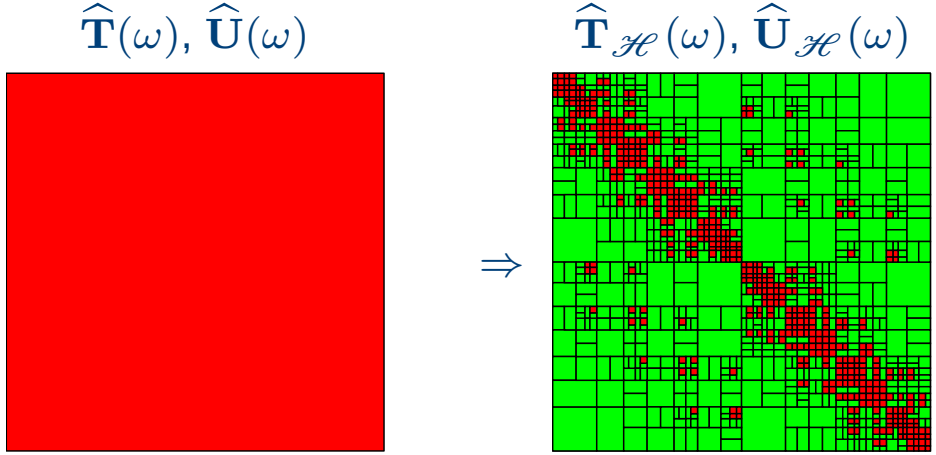

- The modified BE equations are solved with an iterative GMRES–solver:

$$\widehat{\mathbf{U}}_{\mathscr{H}}(\omega)\underline{\hat{\mathbf{t}}}(\omega) = \left[\widehat{\mathbf{T}}_{\mathscr{H}}(\omega) + \mathbf{I}\right] \underline{\hat{\mathbf{u}}}(\omega)$$

- Example: surface foundation on a layered halfspace

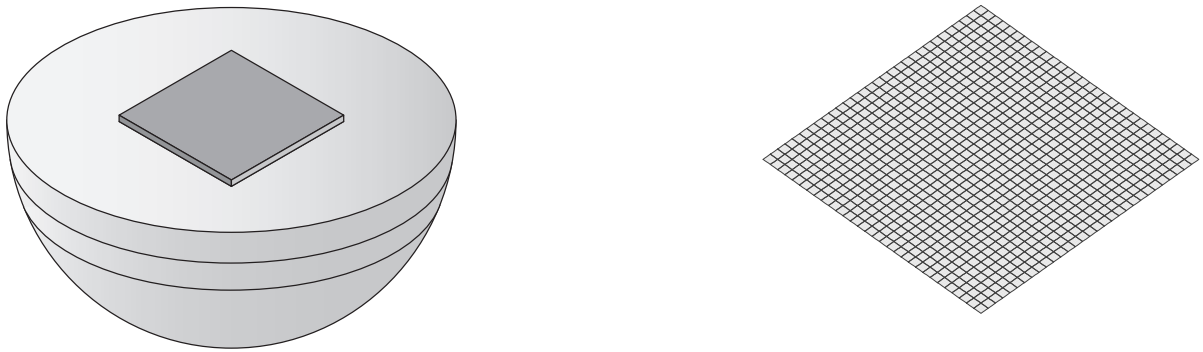

3D BE method based on $\mathscr{H}$–matrices

- Hierarchical clustering (based on principal component analysis) [Bebendorf, SPRINGER, 2008]:

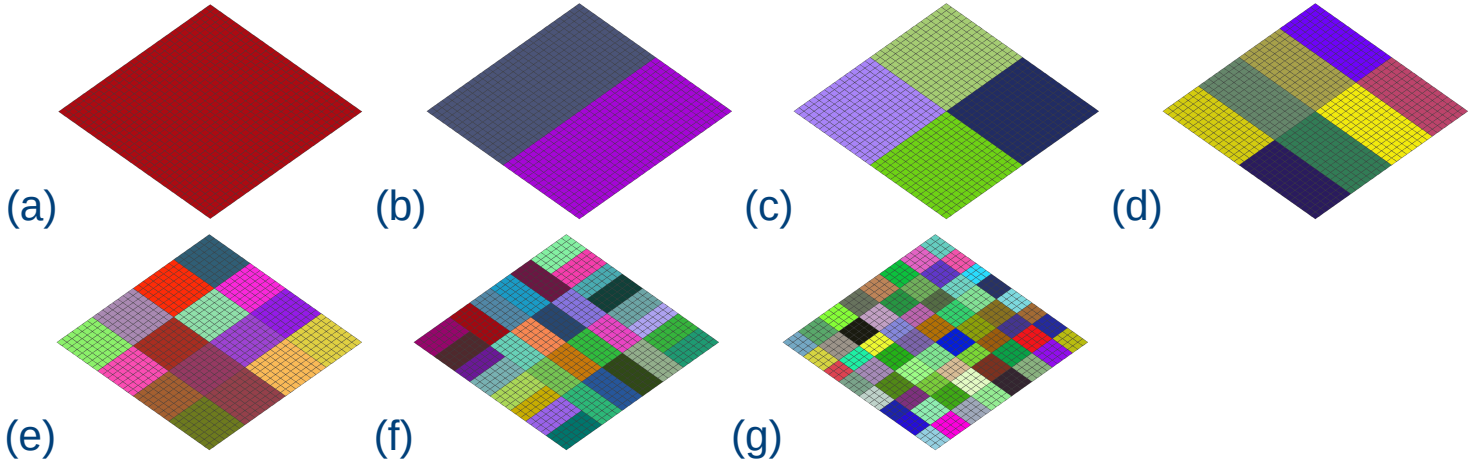

- Identification of (in)admissible cluster pairs:
  - Red blocks (inadmissible pairs): computed exactly
  - Green blocks (admissible pairs): low rank approximations (SVD, ACA, . . .)

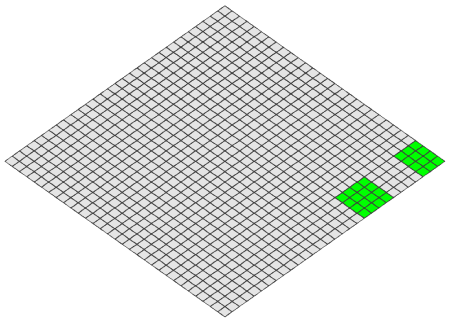

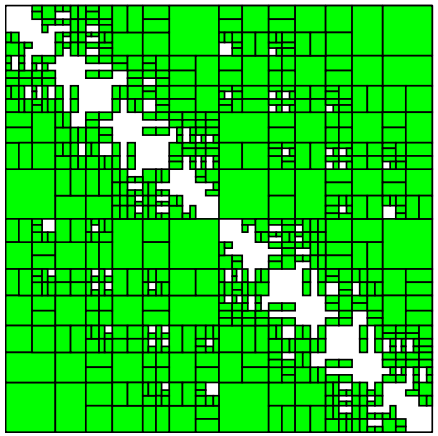

3D BE method based on $\mathscr{H}$–matrices

- Hierarchical clustering (based on principal component analysis) [Bebendorf, SPRINGER, 2008]:

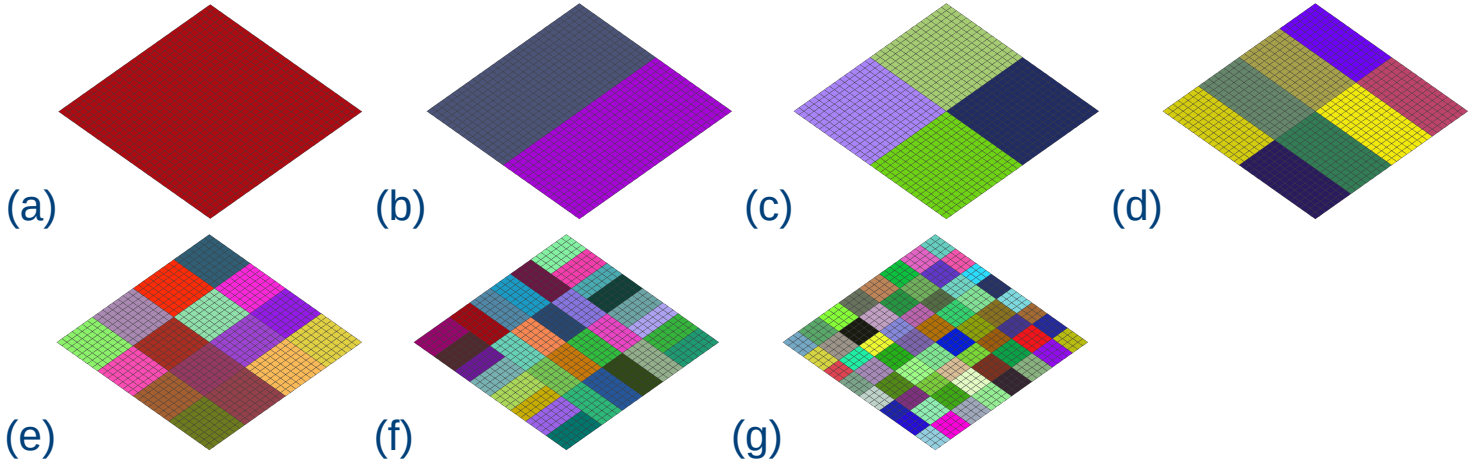

- Identification of (in)admissible cluster pairs:
  - Red blocks (inadmissible pairs): computed exactly
  - Green blocks (admissible pairs): low rank approximations (SVD, ACA, . . .)

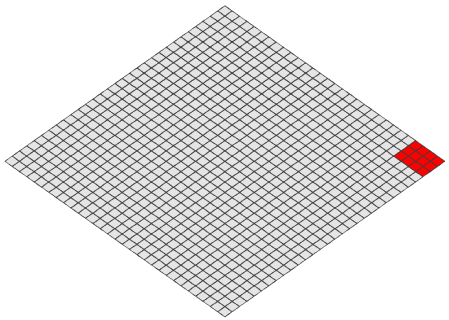

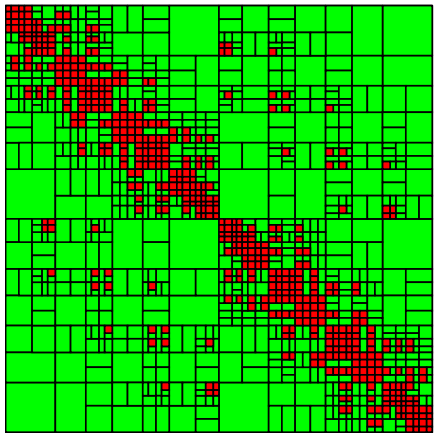

3D BE method based on $\mathscr{H}$–matrices

- Low rank approximation using Adaptive Cross Approximation ($k \ll m, n$) [Bebendorf and Rjasanow, COMPUTING, 2003]:

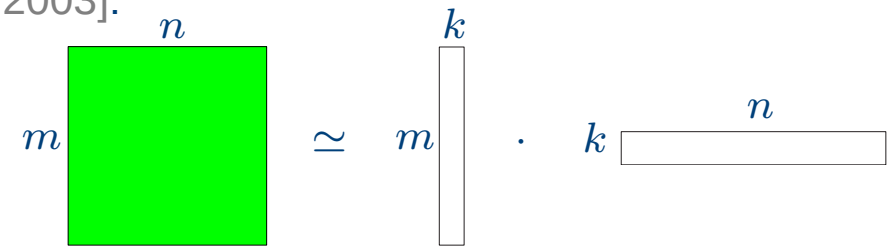

$\Rightarrow$ memory reduction: $\mathcal{O}(mn) \rightarrow \mathcal{O}(k(m+n))$

$\Rightarrow$ fast matrix–vector multiplication: $\mathcal{O}(2mn) \rightarrow \mathcal{O}(2k(m+n)-k)$

- Soil impedance of a surface foundation on a layered halfspace: (a) memory and (b) CPU time

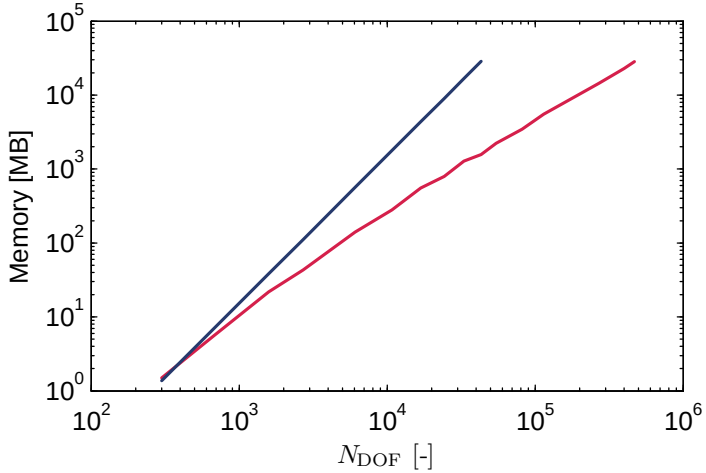

(a)

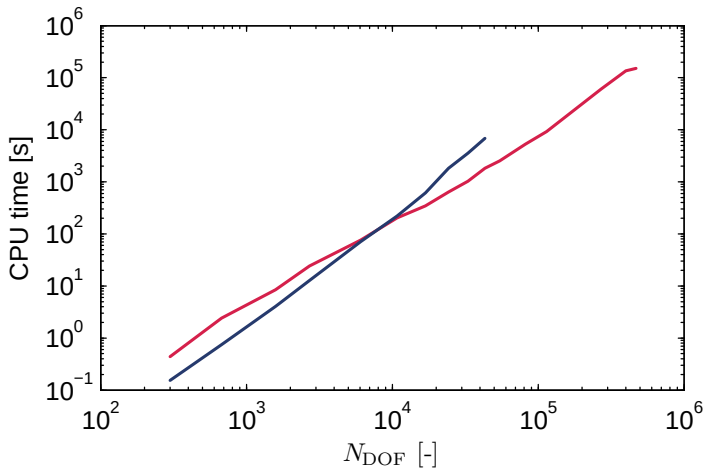

(b)

N_{DOF} [–]	BEM [GB]	$\mathscr{H}$–BEM [GB]	% [–]
43200	28	1.9	7.1 %
468075	(3265)	28	0.8 %

3D BE method based on $\mathscr{H}$–matrices

- Example: surface foundation on a layered halfspace

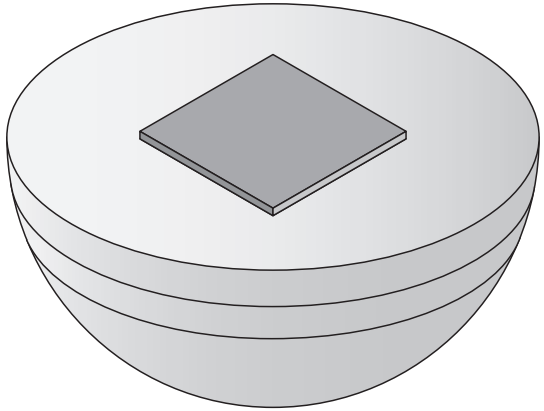

  - $a_0 = \omega B/C_s = 2.5$ (left) and $a_0 = \omega B/C_s = 10$ (right)

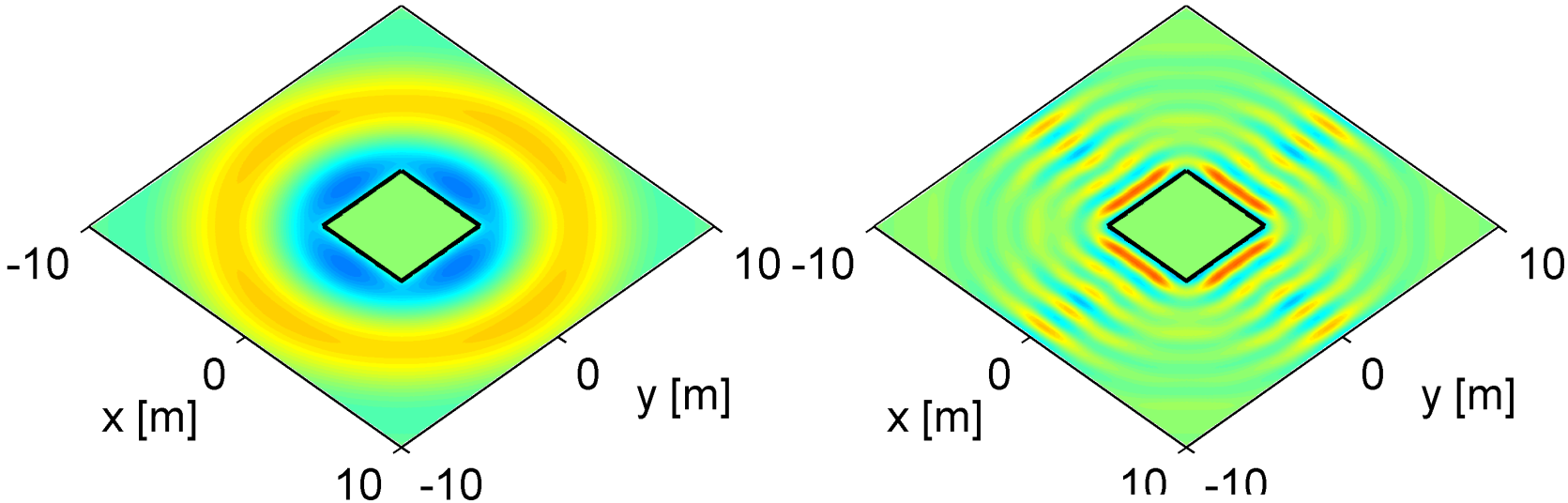

3D BE method based on $\mathscr{H}$–matrices

- Example: semi–spherical canyon subjected to a vertically incident plane P–wave

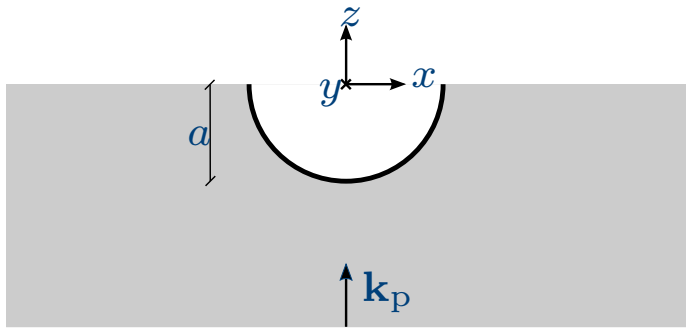

- $\bar{f}_\mathrm{p} = k_\mathrm{p} a/\pi = 2a/\lambda_\mathrm{p} = 0.5$

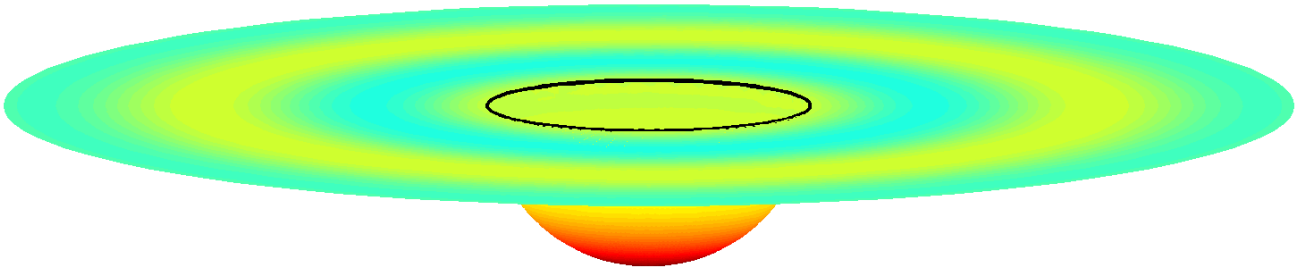

- $\bar{f}_\mathrm{p} = k_\mathrm{p} a/\pi = 2a/\lambda_\mathrm{p} = 5$

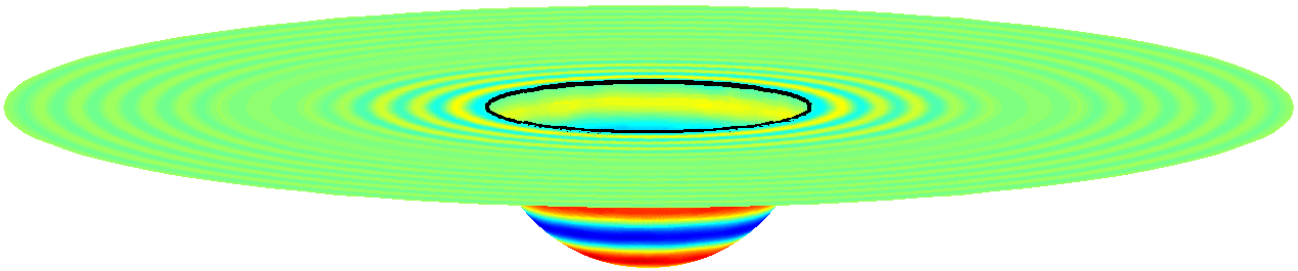

FE–$\mathscr{H}$-BE coupling methodologies

- Three FE–$\mathscr{H}$-BE coupling methodologies have been investigated
- Direct coupling: influence of the soil is condensed into a dynamic soil stiffness matrix $\hat{\mathbf{K}}^{\mathrm{s}}_{22}(\omega)$ [Von Estorff et al., EESD, 1989]:

$$\left(\begin{bmatrix} \widehat{\mathbf{K}}_{11}(\omega) & \widehat{\mathbf{K}}_{12}(\omega) \\ \widehat{\mathbf{K}}_{21}(\omega) & \widehat{\mathbf{K}}_{22}(\omega) \end{bmatrix} + \begin{bmatrix} \mathbf{0} & \mathbf{0} \\ \mathbf{0} & \widehat{\mathbf{K}}^{\mathrm{s}}_{22}(\omega) \end{bmatrix} \right) \begin{Bmatrix} \underline{\hat{\mathbf{u}}}_1(\omega) \\ \underline{\hat{\mathbf{u}}}_2(\omega) \end{Bmatrix} = \begin{Bmatrix} \underline{\hat{\mathbf{f}}}_1(\omega) \\ \underline{\hat{\mathbf{f}}}_2(\omega) \end{Bmatrix} + \begin{Bmatrix} \mathbf{0} \\ \underline{\hat{\mathbf{f}}}^{\mathrm{s}}_2(\omega) \end{Bmatrix}$$

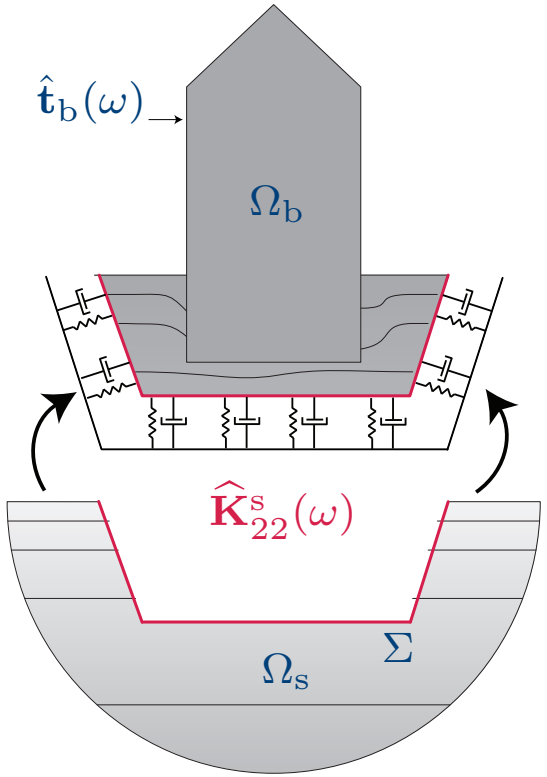

- Dynamic soil stiffness matrix $\hat{\mathbf{K}}^{\mathrm{s}}_{22}(\omega)$:

$$\begin{aligned} \widehat{\mathbf{K}}^{\mathrm{s}}_{22}(\omega) &= \int_{\Sigma} \mathbf{N}^{\mathrm{T}}(\mathbf{x}) \mathbf{N}(\mathbf{x}) \underline{\hat{\mathbf{t}}}(\mathbf{N}(\mathbf{x}))(\omega) \, \mathrm{d}S \\ &= \mathbf{T}_{\mathrm{q}} \, \underline{\hat{\mathbf{t}}}(\mathbf{N}(\mathbf{x}))(\omega) \end{aligned}$$

FE–$\mathscr{H}$-BE coupling methodologies

- Iterative coupling: governing equations are solved separately for each subdomain; boundary conditions at Σ are updated until convergence is achieved
  - *Sequential Neumann–Dirichlet*
  - Sequential Dirichlet–Neumann
  - Parallel Neumann–Neumann
  - Parallel Dirichlet–Dirichlet

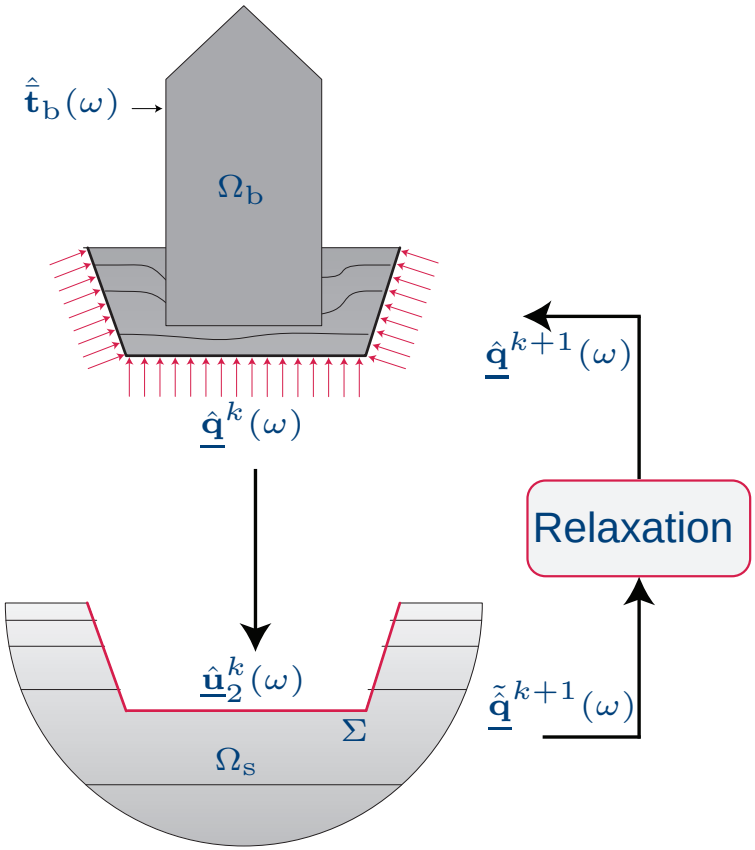

1. FE subdomain: Neumann boundary conditions at the interface Σ (soil–structure interaction forces $\underline{\hat{\mathbf{q}}}^{k}(\omega)$)
   $\Rightarrow$ displacements $\underline{\hat{\mathbf{u}}}_1^{k}(\omega)$ and $\underline{\hat{\mathbf{u}}}_2^{k}(\omega)$
2. BE subdomain: Dirichlet boundary conditions ($\underline{\hat{\mathbf{u}}}_2^{k}(\omega)$)
   $\Rightarrow$ equivalent nodal forces $\underline{\hat{\mathbf{q}}}^{k+\lambda}(\omega)$:
3. The interaction forces are finally relaxed using a relaxation parameter λ^{k}:

$$\underline{\hat{\mathbf{q}}}^{k+1}(\omega) = \lambda^{k}\underline{\hat{\mathbf{q}}}^{k+\lambda}(\omega) + (1-\lambda^{k})\underline{\hat{\mathbf{q}}}^{k}(\omega)$$

FE–$\mathscr{H}$-BE coupling methodologies

- Surface foundation on a layered halfspace excited at $50\,\mathrm{Hz}$

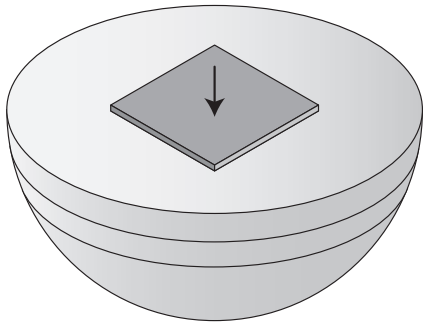

- Sequential Neumann–Dirichlet procedure:
  - Displacements $\underline{\hat{\mathbf{u}}}(\omega)$

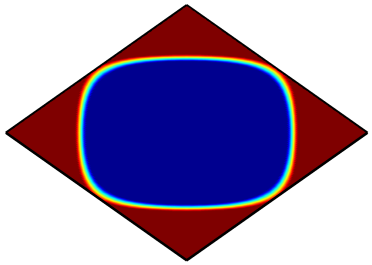

  - Tractions $\underline{\hat{\mathbf{t}}}(\omega)$

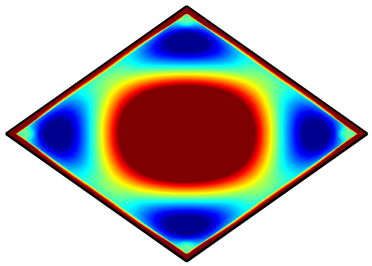

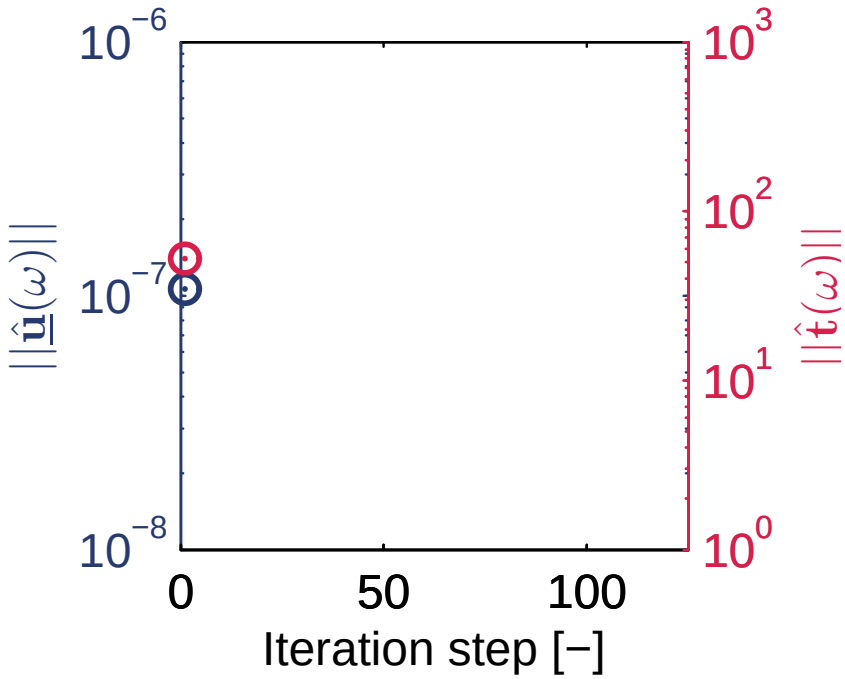

FE–$\mathscr{H}$-BE coupling methodologies

- Iterative coupling:
  - Not often used in the *frequency domain* due to convergence difficulties [Soares et al., COMPUT STRUCT, 2012]
  - Interface relaxation is crucial: Aitken's Δ^2–method [Aitken, PRSE, 1937]

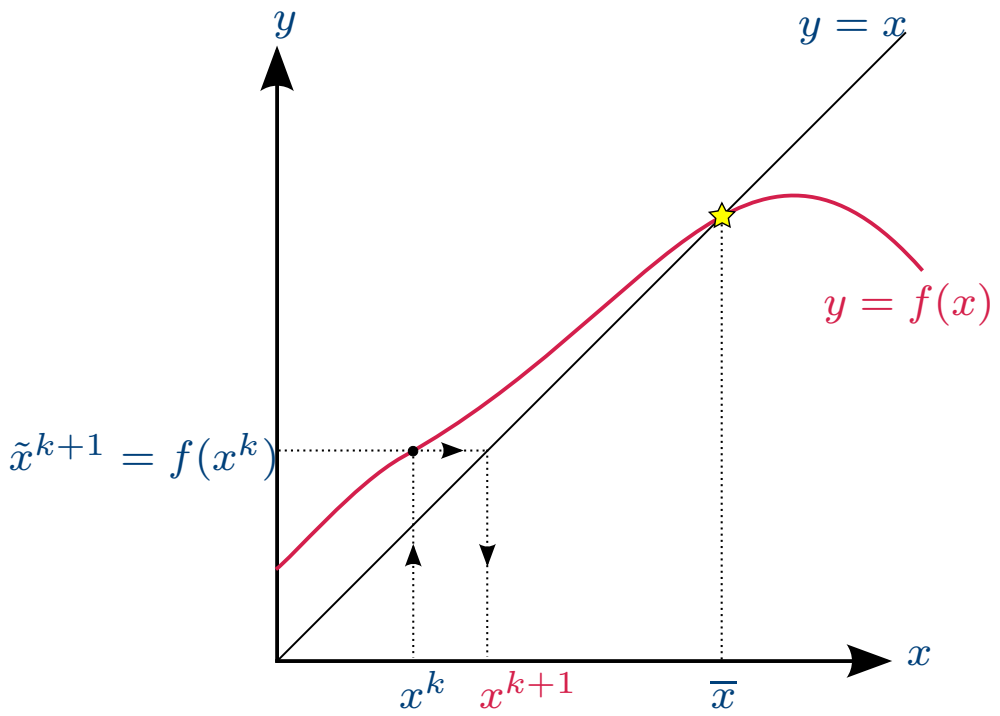

  - Recursive vector implementation presented by Irons and Tuck is used [Irons and Tuck, IJNME, 1969]
  - Efficiency depends on the type of boundary conditions imposed on each subdomain

FE–$\mathscr{H}$-BE coupling methodologies

- Iterative coupling:
  - Not often used in the *frequency domain* due to convergence difficulties [Soares et al., COMPUT STRUCT, 2012]
  - Interface relaxation is crucial: Aitken's Δ^2–method [Aitken, PRSE, 1937]

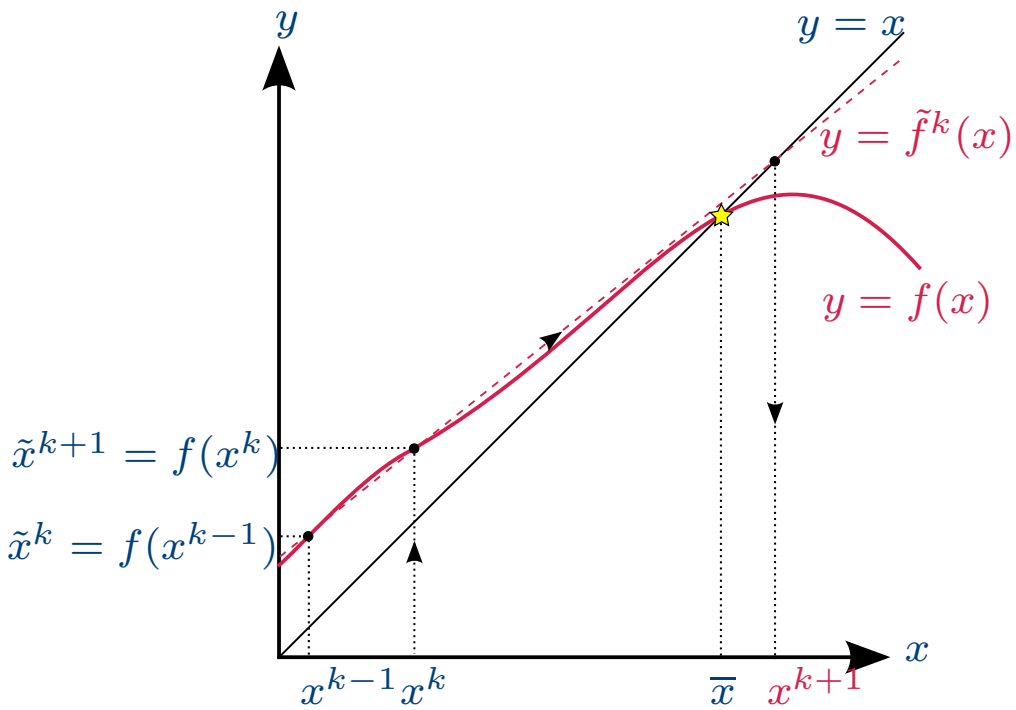

  - Recursive vector implementation presented by Irons and Tuck is used [Irons and Tuck, IJNME, 1969]
  - Efficiency depends on the type of boundary conditions imposed on each subdomain

FE–$\mathscr{H}$-BE coupling methodologies

- Iterative coupling:
  - Not often used in the *frequency domain* due to convergence difficulties [Soares et al., COMPUT STRUCT, 2012]
  - Interface relaxation is crucial: Aitken's Δ^2–method [Aitken, PRSE, 1937]
  - Recursive vector implementation presented by Irons and Tuck is used [Irons and Tuck, IJNME, 1969]
  - Efficiency depends on the type of boundary conditions imposed on each subdomain

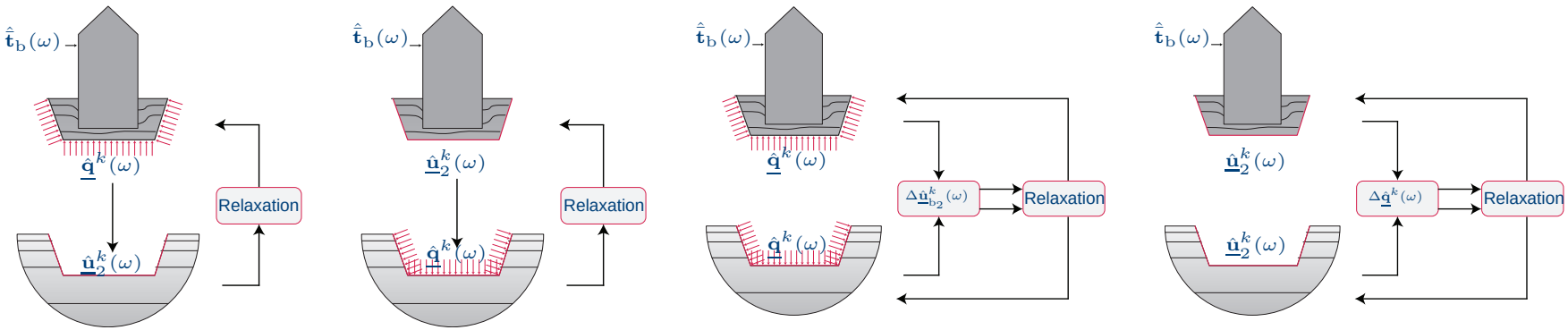

FE–$\mathscr{H}$-BE coupling methodologies

- Monolithic coupling:
  - Used for the solution of strongly coupled fluid–structure interaction problems [Hübner et al., COMPUT METHOD APPL M, 2004; Michler et al., COMPUT FLUIDS, 2004]
  - Governing equations of both subdomains are solved simultaneously, although the BE method is not forced into an FE frame:

$$\begin{bmatrix} \widehat{\mathbf{K}}_{11}(\omega) & \widehat{\mathbf{K}}_{12}(\omega) & \mathbf{0} \\ \widehat{\mathbf{K}}_{21}(\omega) & \widehat{\mathbf{K}}_{22}(\omega) & \mathbf{T}_{\mathrm{q}} \\ \mathbf{0} & \widehat{\mathbf{T}}_{\mathscr{H}}(\omega) + \mathbf{I} & -\widehat{\mathbf{U}}_{\mathscr{H}}(\omega) \end{bmatrix} \begin{Bmatrix} \underline{\hat{\mathbf{u}}}_1(\omega) \\ \underline{\hat{\mathbf{u}}}_2(\omega) \\ \underline{\hat{\mathbf{t}}}(\omega) \end{Bmatrix} = \begin{Bmatrix} \underline{\hat{\mathbf{f}}}_1(\omega) \\ \underline{\hat{\mathbf{f}}}_2(\omega) \\ \underline{\mathbf{0}} \end{Bmatrix} + \begin{Bmatrix} \underline{\mathbf{0}} \\ \underline{\hat{\mathbf{f}}}_2^{\mathrm{s}}(\omega) \\ \underline{\mathbf{0}} \end{Bmatrix}$$

  - The set of equations is solved iteratively by means of GMRES (coefficient matrix is never assembled explicitly) $\Rightarrow$ only advantageous if a fast BE method (i.c. a hierarchical formulation) is employed, enabling an efficient matrix–vector multiplication
  - Preconditioning is crucial: block diagonal right preconditioner (FGMRES) is incorporated in the implementation

FE–$\mathscr{H}$-BE coupling methodologies

- Homogeneous full space ($C_\mathrm{s} = 150\,\mathrm{m/s}$; $C_\mathrm{p} = 300\,\mathrm{m/s}$; $\rho = 1800\,\mathrm{kg/m^3}$; $\beta_\mathrm{s} = \beta_\mathrm{p} = 0.025$)
- Spherical layer (inner radius $r_\mathrm{i} = 1\,\mathrm{m}$, outer radius $r_\mathrm{o} = 2\,\mathrm{m}$) loaded by an internal pressure $\hat{p}(\omega) = 1\,\mathrm{Pa/Hz}$.
  - αC_s; αC_p; $\rho = 1800\,\mathrm{kg/m^3}$; $\beta_\mathrm{s} = \beta_\mathrm{p} = 0.025$.
  - Following values are considered for the factor α: (a) $\alpha = 1/2$, (b) $\alpha = 1$, and (c) $\alpha = 2$.

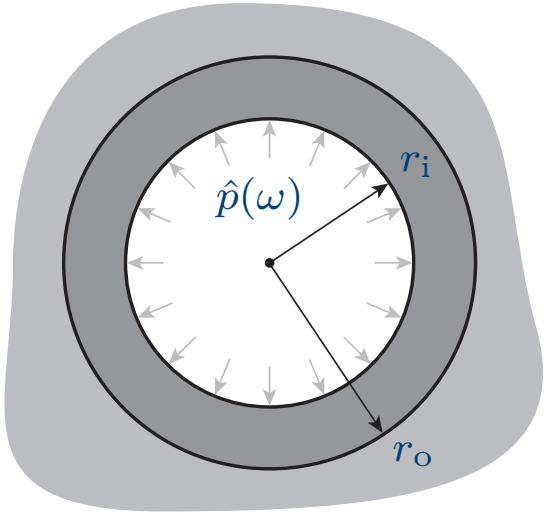

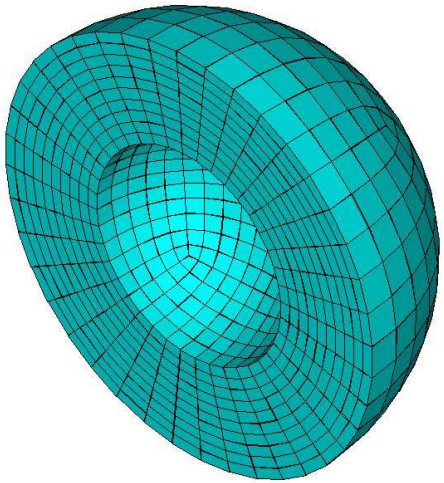

- FE–BE discretization:
  - Spherical layer: 6000 eight node solid finite elements (19866 FE DOFs)
  - Full space: 600 conforming four node quadrilateral boundary elements (1806 BE DOFs)

FE–$\mathscr{H}$-BE coupling methodologies

- CPU time required in the direct, iterative Neumann–Dirichlet, Dirichlet–Neumann, Neumann–Neumann and Dirichlet–Dirichlet, and monolithic coupling strategies
  - $\alpha = 1/2$

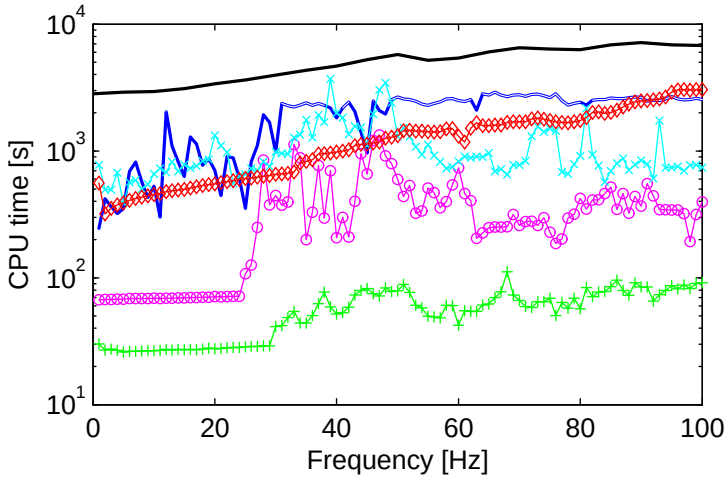

  - $\alpha = 1$

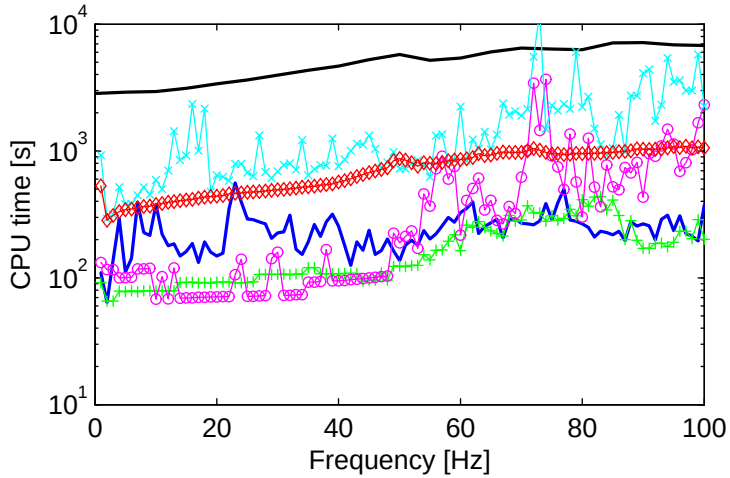

  - $\alpha = 2$

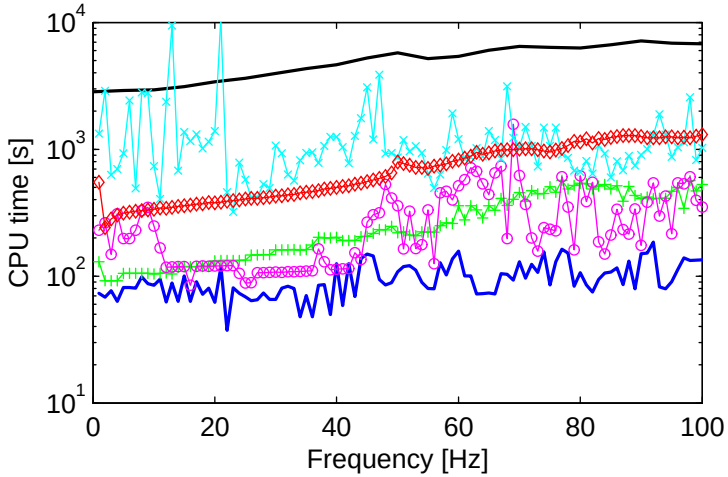

2.5D FE–BE method with spatial windowing

- Three–dimensional (3D) formulations: complex geometries, but computationally expensive
- Two–and–a–half–dimensional (2.5D) formulations for structures with a longitudinally invariant geometry: pipelines, dams, roads, railway tracks, tunnels, . . .

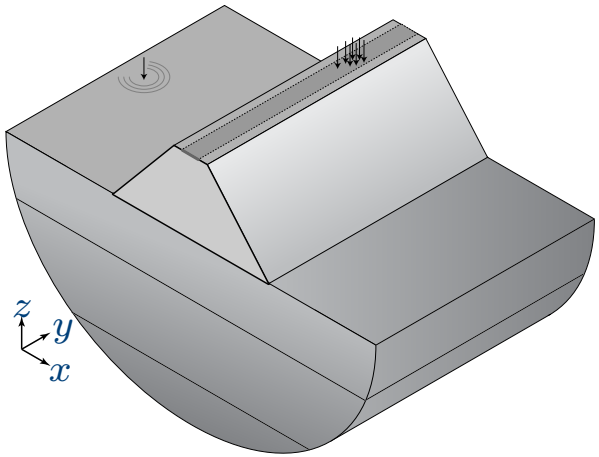

2.5D FE–BE method with spatial windowing

- Three–dimensional (3D) formulations: complex geometries, but computationally expensive
- Two–and–a–half–dimensional (2.5D) formulations for structures with a longitudinally invariant geometry: pipelines, dams, roads, railway tracks, tunnels, . . .

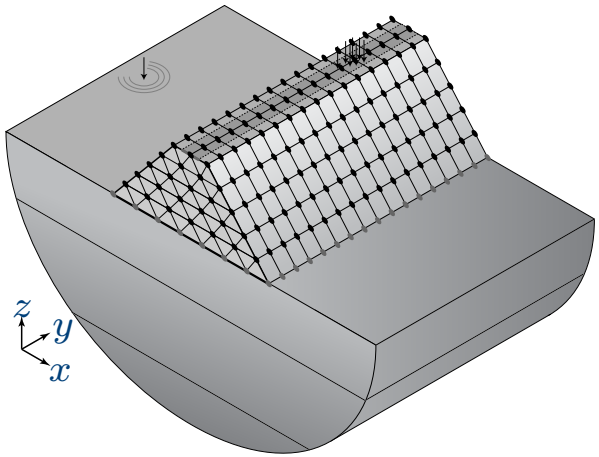

2.5D FE–BE method with spatial windowing

- Three–dimensional (3D) formulations: complex geometries, but computationally expensive
- Two–and–a–half–dimensional (2.5D) formulations for structures with a longitudinally invariant geometry: pipelines, dams, roads, railway tracks, tunnels, . . .

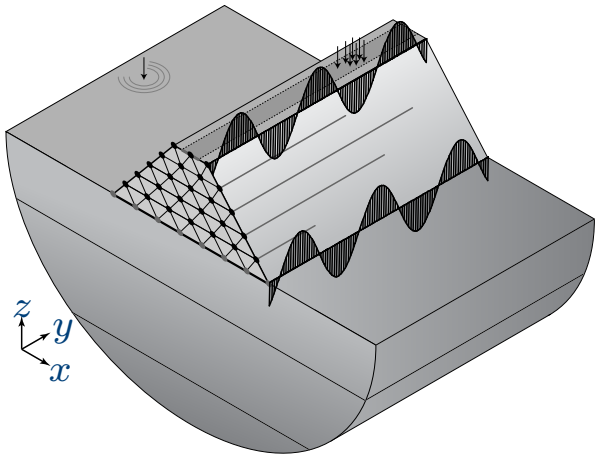

2.5D FE–BE method with spatial windowing

- Computationally efficient 2.5D approach in the frequency–wavenumber domain:
  - Forward Fourier transform from y to k_y: $\mathscr{F}\left[f(y), k_y\right] = \int_{-\infty}^{+\infty} f(y) \exp\left(ik_y y\right) \, \mathrm{d}y$
  - 2.5D FE [Gavríc, J SOUND VIB, 1994], 2.5D BE [Stamos and Beskos, SOIL DYN EARTHQ ENG, 1996], 2.5D FE–BE [François et al., COMPUT METHOD APPL M, 2010], 2.5D FE–PML [François et al., INT J NUMER METH ENG, 2012], ...

$$\left[\tilde{\mathbf{K}}_{\mathrm{b}}(k_y,\omega) + \mathbf{C}_{\mathrm{b}} - \omega^2\mathbf{M}_{\mathrm{b}} + \tilde{\mathbf{K}}^{\mathrm{s}}_{\mathrm{b}}(k_y,\omega)\right] \underline{\tilde{\mathbf{u}}}_{\mathrm{b}}(k_y,\omega) = \underline{\tilde{\mathbf{f}}}_{\mathrm{b}}(k_y,\omega) + \underline{\tilde{\mathbf{f}}}^{\mathrm{s}}_{\mathrm{b}}(k_y,\omega)$$

  - Inverse Fourier transform from k_y to y: $\mathscr{F}^{-1}\left[f(k_y), y\right] = \frac{1}{2\pi} \int_{-\infty}^{+\infty} f(k_y) \exp\left(-ik_y y\right) \, \mathrm{d}k_y$

- The assumption of longitudinal invariance might be too restrictive in some cases
  $\Rightarrow$ a 3D analysis is required to account for the structure's finite length

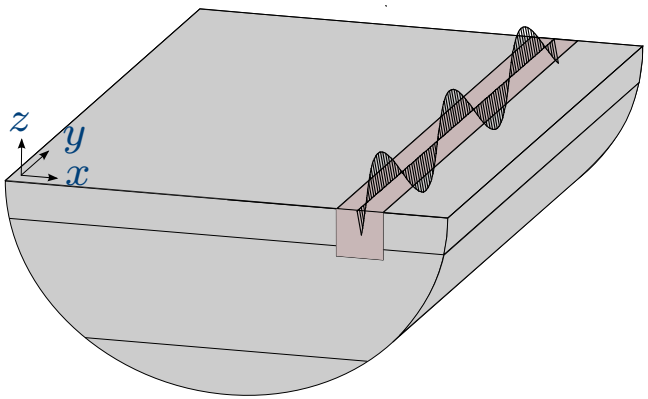

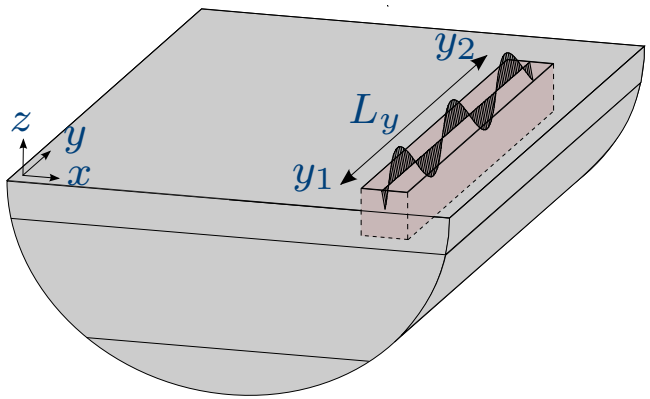

2.5D FE–BE method with spatial windowing

- Spatial windowing technique: accounts for the structure's finite length, while maintaining the computational efficiency of a 2.5D approach
- Plane wave with a constant longitudinal wavenumber k_{y0}: $\hat{u}(y,\omega) = \frac{1}{2\pi}\hat{u}_0(\omega)\exp\left(-ik_{y0}y\right)$
  - Structure of infinite length [Stamos and Beskos, SOIL DYN EARTHQ ENG, 1996; François et al., COMPUT METHOD APPL M, 2010; many others]

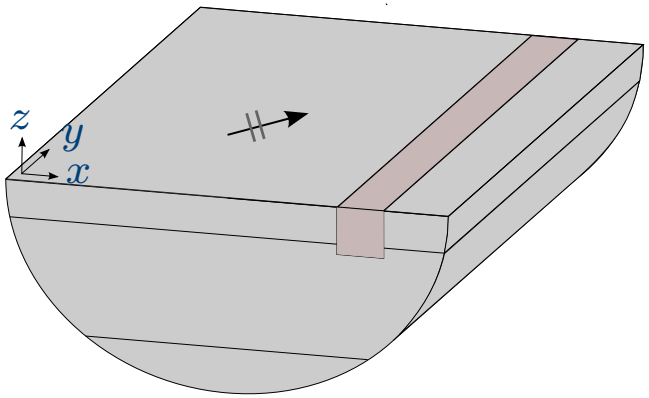

$$\tilde{u}(k_y,\omega) = \int_{-\infty}^{+\infty} \frac{1}{2\pi}\hat{u}_0(\omega)\exp\left(-ik_{y0}y\right)\exp\left(ik_y y\right)\,\mathrm{d}y$$

$$= \hat{u}_0(\omega)\delta\left(k_y - k_{y0}\right)$$

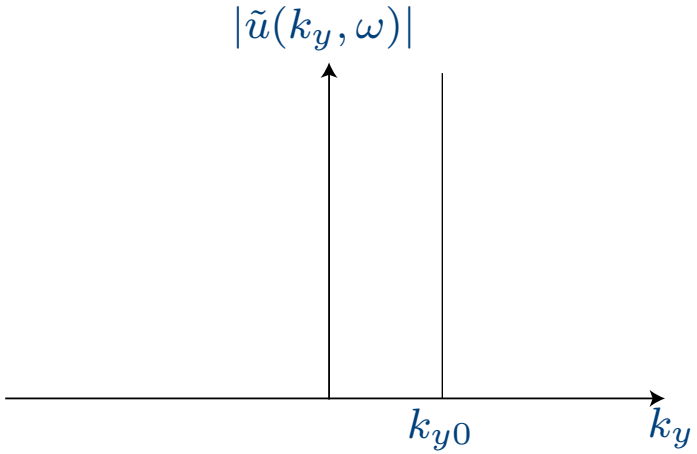

2.5D FE–BE method with spatial windowing

- Spatial windowing technique: accounts for the structure's finite length, while maintaining the computational efficiency of a 2.5D approach
- Plane wave with a constant longitudinal wavenumber k_{y0}: $\hat{u}(y,\omega) = \frac{1}{2\pi}\hat{u}_0(\omega)\exp\left(-ik_{y0}y\right)$
  - Structure of finite length L_y (from y_1 to y_2) [Villot et al., J SOUND VIB, 2001; Legault et al., J SOUND VIB, 2011]

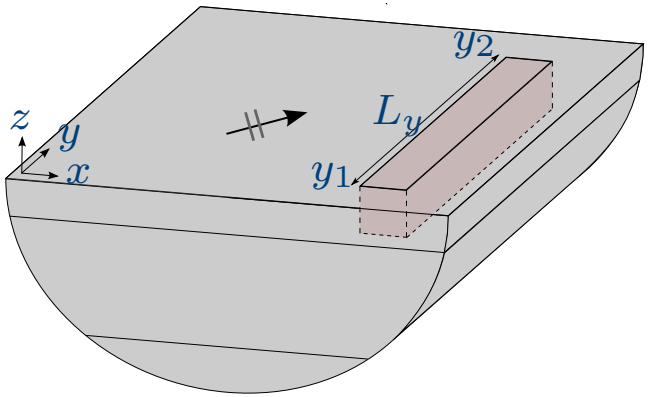

$$\tilde{u}_{\mathrm{sw}}(k_y,\omega) = \int_{y_1}^{y_2} \frac{1}{2\pi}\hat{u}_0(\omega)\exp\left(-ik_{y0}y\right)\exp\left(ik_y y\right)\,\mathrm{d}y$$

$$= \frac{1}{2\pi}\hat{u}_0(\omega)\frac{\exp\left[i\left(k_y-k_{y0}\right)y_2\right]}{i\left(k_y-k_{y0}\right)}\left(1-\exp\left[-i\left(k_y-k_{y0}\right)L_y\right]\right)$$

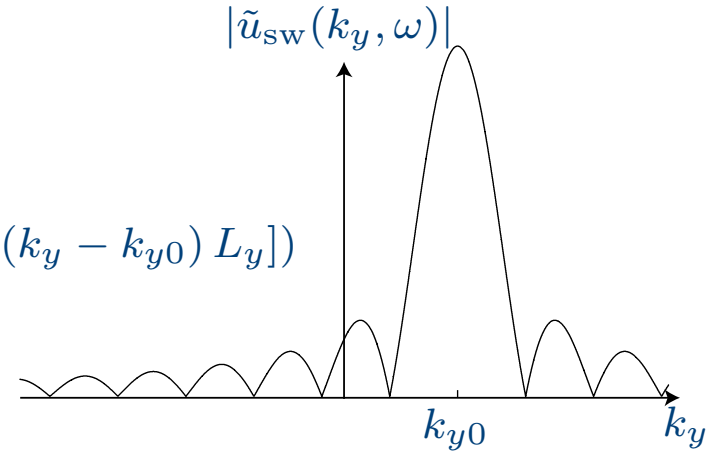

2.5D FE–BE method with spatial windowing

- Spatial windowing technique accounts for the structure's finite length, while maintaining the computational efficiency of a 2.5D approach:
- Redistribution of the wavenumber spectrum over the entire wavenumber domain [Villot et al., J SOUND VIB, 2001; Legault et al., J SOUND VIB, 2011]:

$$\tilde{f}_{\mathrm{sw}}(k_y) = \int_{y_1}^{y_2} f(y) \exp\left(ik_y y\right) \, \mathrm{d}y = \tilde{f}(k_y) * \tilde{w}\left(k_y\right)$$

- Windowing function $\tilde{w}\left(k_y\right)$:

$$\tilde{w}\left(k_y\right) = \int_{y_1}^{y_2} \frac{1}{2\pi} \exp\left(ik_y y\right) \, \mathrm{d}y = \left[\frac{1}{2\pi} \frac{\exp\left(ik_y y_2\right)}{ik_y} \left(1 - \exp\left[-ik_y L_y\right]\right)\right]$$

$$\left|\tilde{w}\left(k_y\right)\right|$$

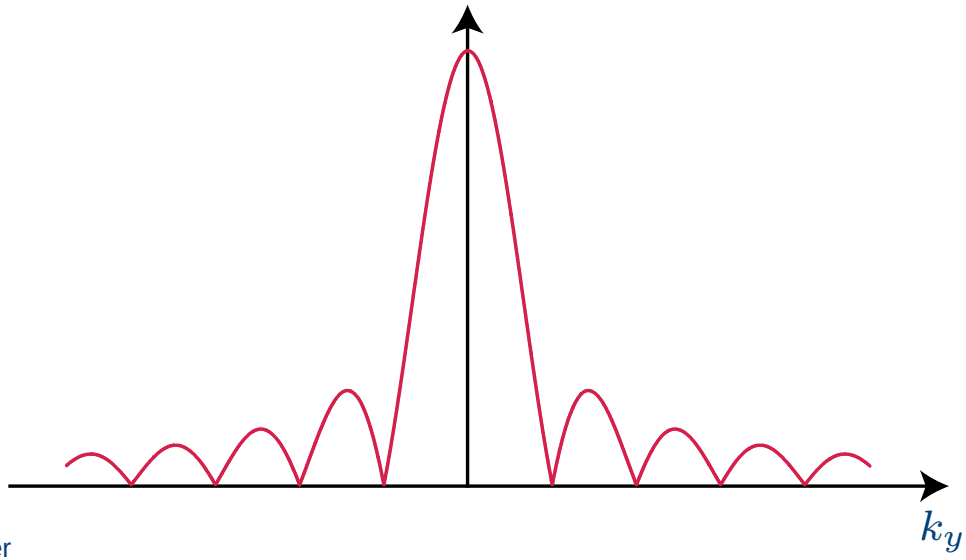

2.5D FE–BE method with spatial windowing

- Open trench of $2\,\mathrm{m} \times 2\,\mathrm{m}$ in a homogeneous halfspace
- Vertical displacement $\hat{u}_z(\mathbf{x}, \omega)$ at $30\,\mathrm{Hz}$

	2.5D BE (+s.w.)	3D $\mathscr{H}$-BE
$L_y = \infty$	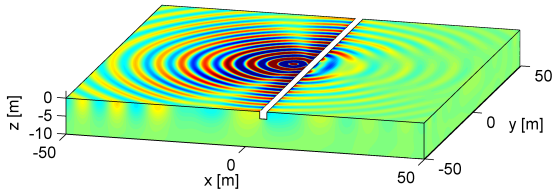	
$L_y = 15\,\mathrm{m}$	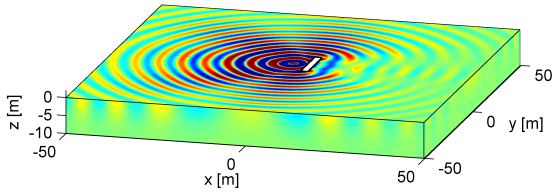 1.10 MB / 0.25 h	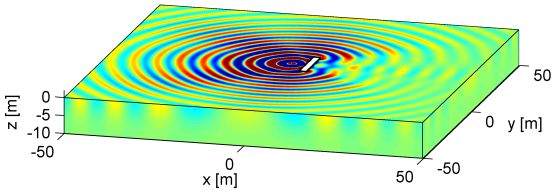 346 MB (736 MB) / 2.0 h
$L_y = 30\,\mathrm{m}$	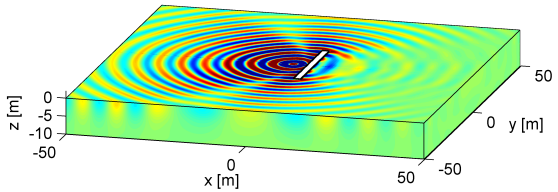 1.10 MB / 0.25 h	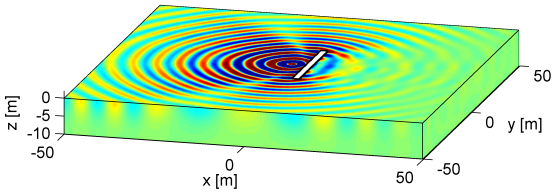 743 MB (2702 MB) / 2.6 h
$L_y = 60\,\mathrm{m}$	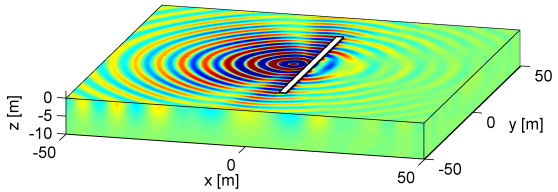 1.10 MB / 0.25 h	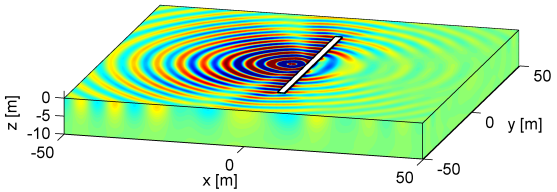 2305 MB (10344 MB) / 4.6 h

2.5D FE–BE method with spatial windowing

- Validation examples for 'elongated' structures:
  - open trench
  - stiff wave barrier
- Also applicable for 'short' structures: surface foundation
  - Vertical displacement $\hat{u}_z(\mathbf{x}, \omega)$ at $100\,\mathrm{Hz}$

2.5D model | 2.5D model with spatial windowing | 3D model

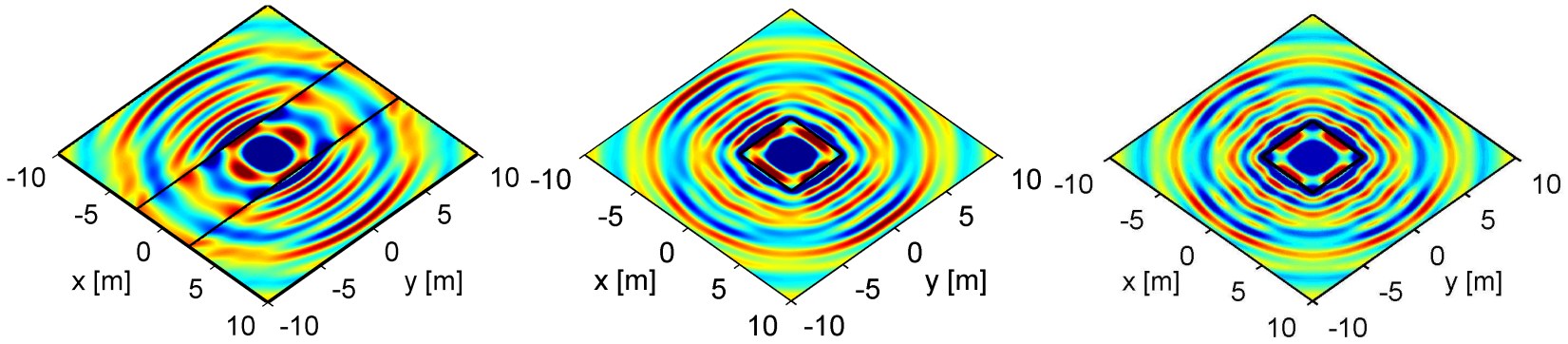

- The technique is appropriate as long as the modal behaviour of the finite structure(s) does not dominate the response

Objectives

- The numerical solution of large 3D dynamic SSI problems remains very challenging and in many cases beyond current computer capabilities
- Fast methods for large scale dynamic SSI problems:
  - 3D BE method based on $\mathscr{H}$–matrices
  - Innovative techniques for the coupling of FE and $\mathscr{H}$-BE models
  - 2.5D FE–BE method with spatial windowing
- Applications related to the prediction of railway induced vibrations:
  - Vibration mitigation measures on the propagation path in the soil
  - Wave propagation in an urban environment
  - The influence of source–receiver interaction

Applications

Railway induced vibrations

- Generation of dynamic axle loads [Knothe and Grassie, VEHICLE SYST DYN, 1993]: wheel and track unevenness, rail joints, parametric excitation, ...
- Wave propagation in the soil
- Vibrations ($1 - 80\,\mathrm{Hz}$) and re–radiated noise ($16 - 250\,\mathrm{Hz}$) in buildings

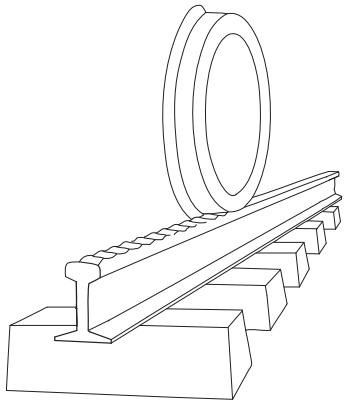

[Thompson, ELSEVIER, 2009]

Consequences of vibrations

- Malfunctioning of sensitive equipment
- Discomfort to people
- (Damage to structures)

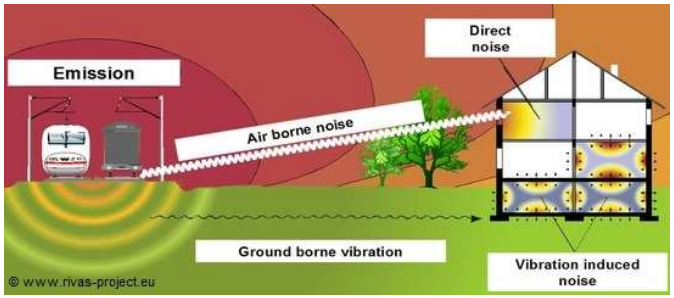

Railway induced vibrations

- Vibration mitigation measures
  - at the source
  - on the propagation path in the soil
    $\Rightarrow$ EU FP7 project RIVAS
  - at the receiver

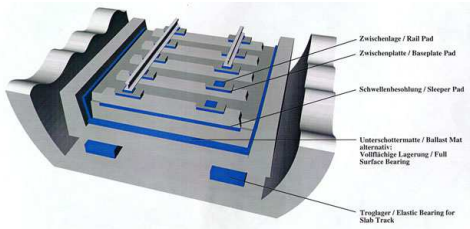

Vibration mitigation measures on the propagation path in the soil

- wave impeding blocks [Takemiya, SOIL DYN EARTHQ ENG, 2004]
- soft wave barriers [Massarsch, GEOFRONTIERS-ASCE, 2005]
- stiff wave barriers [Andersen and Nielsen, SOIL DYN EARTHQ ENG, 2005]

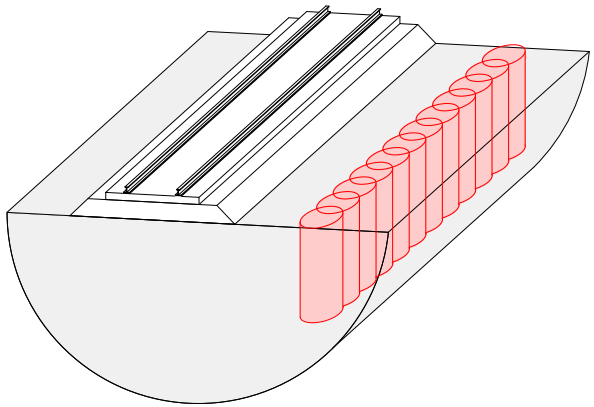

Stiff wave barrier

- Vertical displacement $\hat{u}_z(\mathbf{x},\omega)$ and corresponding insertion loss $\widehat{\mathrm{IL}}_z(\mathbf{x},\omega)$ for a barrier with a length (a) $L_y = \infty$

without barrier | with barrier | insertion loss $\widehat{\mathrm{IL}}_z(\mathbf{x},\omega)$

$$\widehat{\mathrm{IL}}_z(\mathbf{x},\omega) = 20\log_{10}\frac{|\hat{u}_z^{\mathrm{ref}}(\mathbf{x},\omega)|}{|\hat{u}_z(\mathbf{x},\omega)|}$$

- at $30\,\mathrm{Hz}$

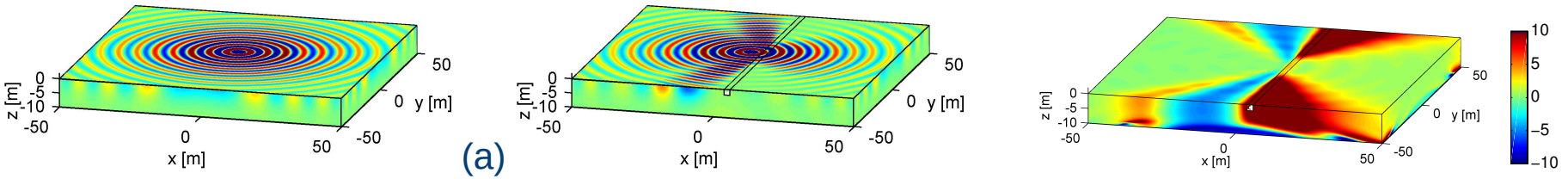

- at $60\,\mathrm{Hz}$

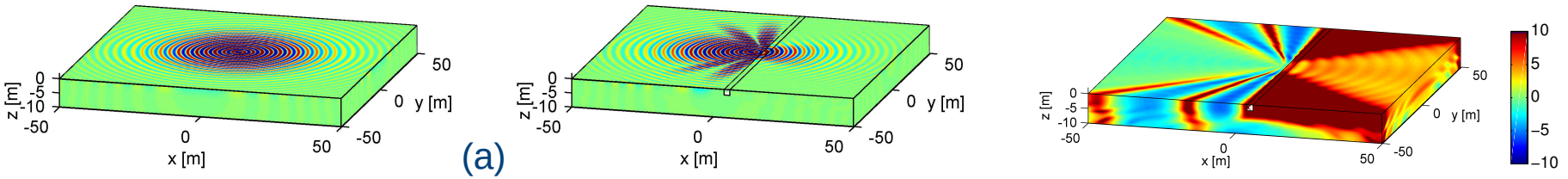

Stiff wave barrier

- Vertical displacement $\hat{u}_z(\mathbf{x},\omega)$ and corresponding insertion loss $\widehat{\mathrm{IL}}_z(\mathbf{x},\omega)$ for a barrier with a length (a) $L_y = \infty$ and (b) $L_y = 15\,\mathrm{m}$

without barrier | with barrier | insertion loss $\widehat{\mathrm{IL}}_z(\mathbf{x},\omega)$

$$\widehat{\mathrm{IL}}_z(\mathbf{x},\omega) = 20\log_{10}\frac{|\hat{u}_z^{\mathrm{ref}}(\mathbf{x},\omega)|}{|\hat{u}_z(\mathbf{x},\omega)|}$$

- at $30\,\mathrm{Hz}$

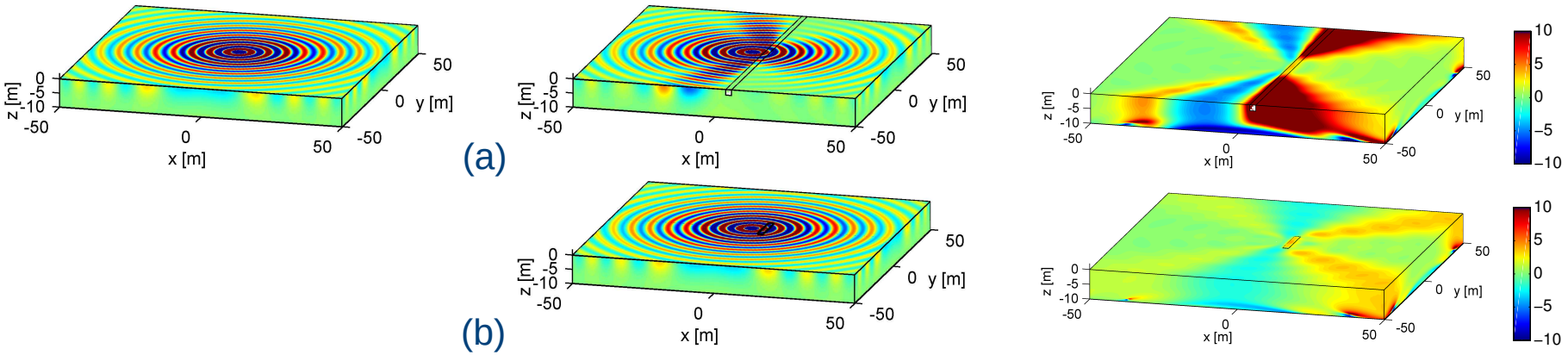

- at $60\,\mathrm{Hz}$

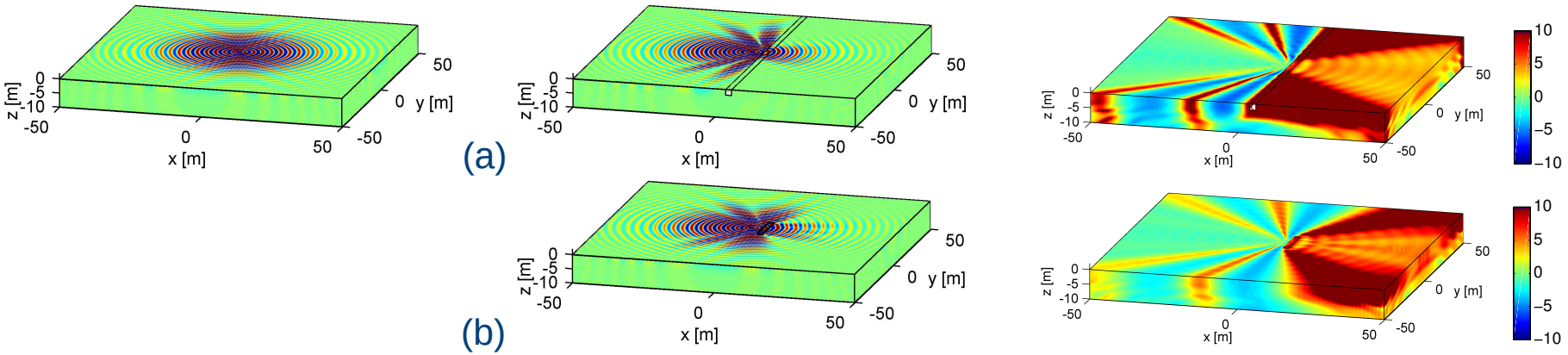

Stiff wave barrier

- Cylindrical wavefield can be decomposed into plane waves, satisfying the dispersion relation $\frac{1}{\lambda_x^2} + \frac{1}{\lambda_y^2} = \frac{1}{\lambda_{\mathrm{R}}^2}$, where $\lambda_{\mathrm{R}} = 2\pi \frac{C_{\mathrm{R}}}{\omega}$ is the Rayleigh wavelength.

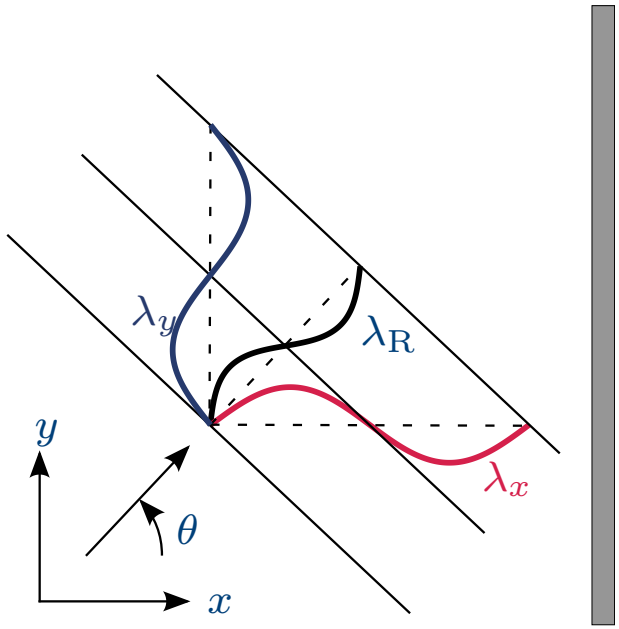

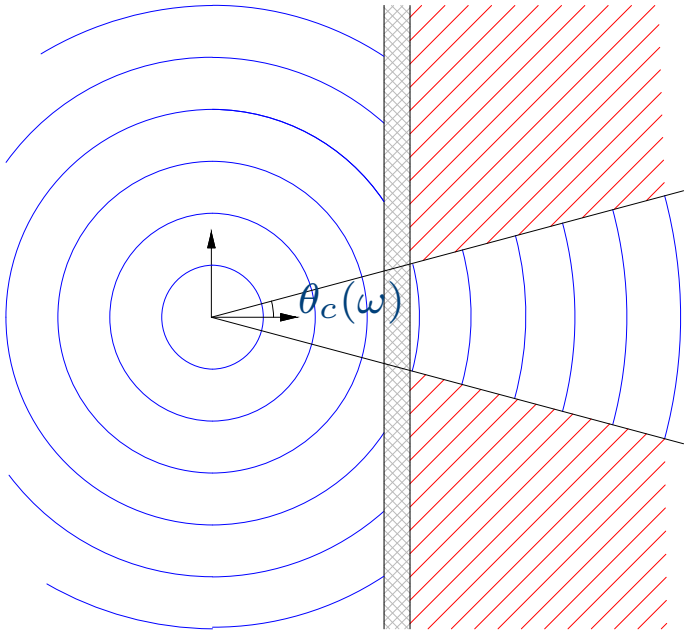

- Euler–Bernoulli beam theory in the (λ_y, ω)-domain:

$$\left(-\rho A \omega^2 + EI \left(\frac{2\pi}{\lambda_y} \right)^4 \right) \tilde{u}_z(\lambda_y, \omega) = \tilde{f}(\lambda_y, \omega)$$

- Free bending wavelength $\lambda_{\mathrm{b}}(\omega)$:

$$\lambda_{\mathrm{b}} = \frac{2\pi}{\sqrt{\omega}} \left(\frac{EI}{\rho A} \right)^{1/4} \Rightarrow \tilde{u}_z(\lambda_y, \omega) \propto 0 \quad \text{for} \quad \lambda_y < \lambda_{\mathrm{b}}$$

Stiff wave barrier

- Vertical insertion loss $\widetilde{\mathrm{IL}}_z(x = 8\,\mathrm{m}, \bar{k}_y, z = 0\,\mathrm{m}, \omega)$ for a barrier with a length (a) $L_y = \infty$ and (b) $L_y = 15\,\mathrm{m}$.

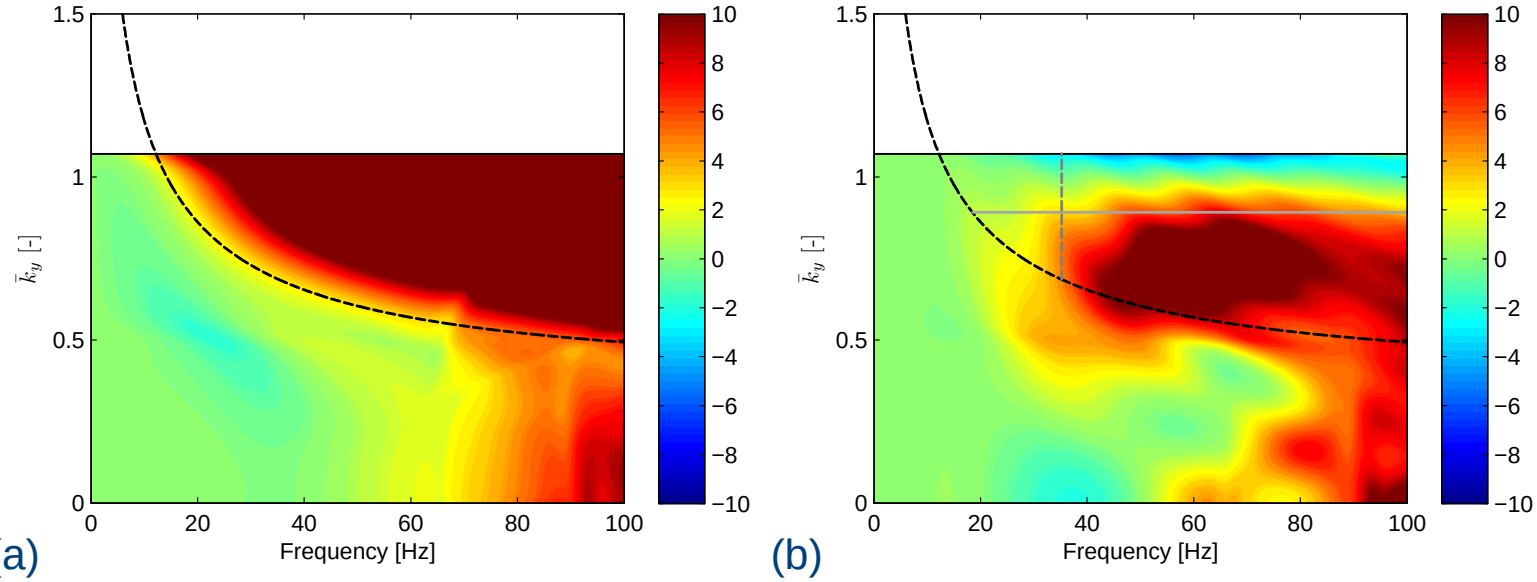

- The transmission of propagating plane waves with a wavenumber $\bar{k}_y$ larger than $\bar{k}_\mathrm{b}(\omega)$ is impeded by the barrier due do its bending stiffness

$\Rightarrow$ Critical frequency $f_\mathrm{c} = \frac{C_\mathrm{R}^2}{2\pi}\sqrt{\frac{\rho A}{EI}}$

$\Rightarrow$ Critical angle $\theta_\mathrm{c}(\omega) = \sin^{-1}\left(\bar{k}_\mathrm{b}(\omega)/\bar{k}_\mathrm{R}(\omega)\right)$

Stiff wave barrier

- Passage of a Renfe S599 train at $160\,\mathrm{km/h}$
- One–third octave band RMS spectra of the vertical free field vibrations *without* and *with* stiff wave barrier

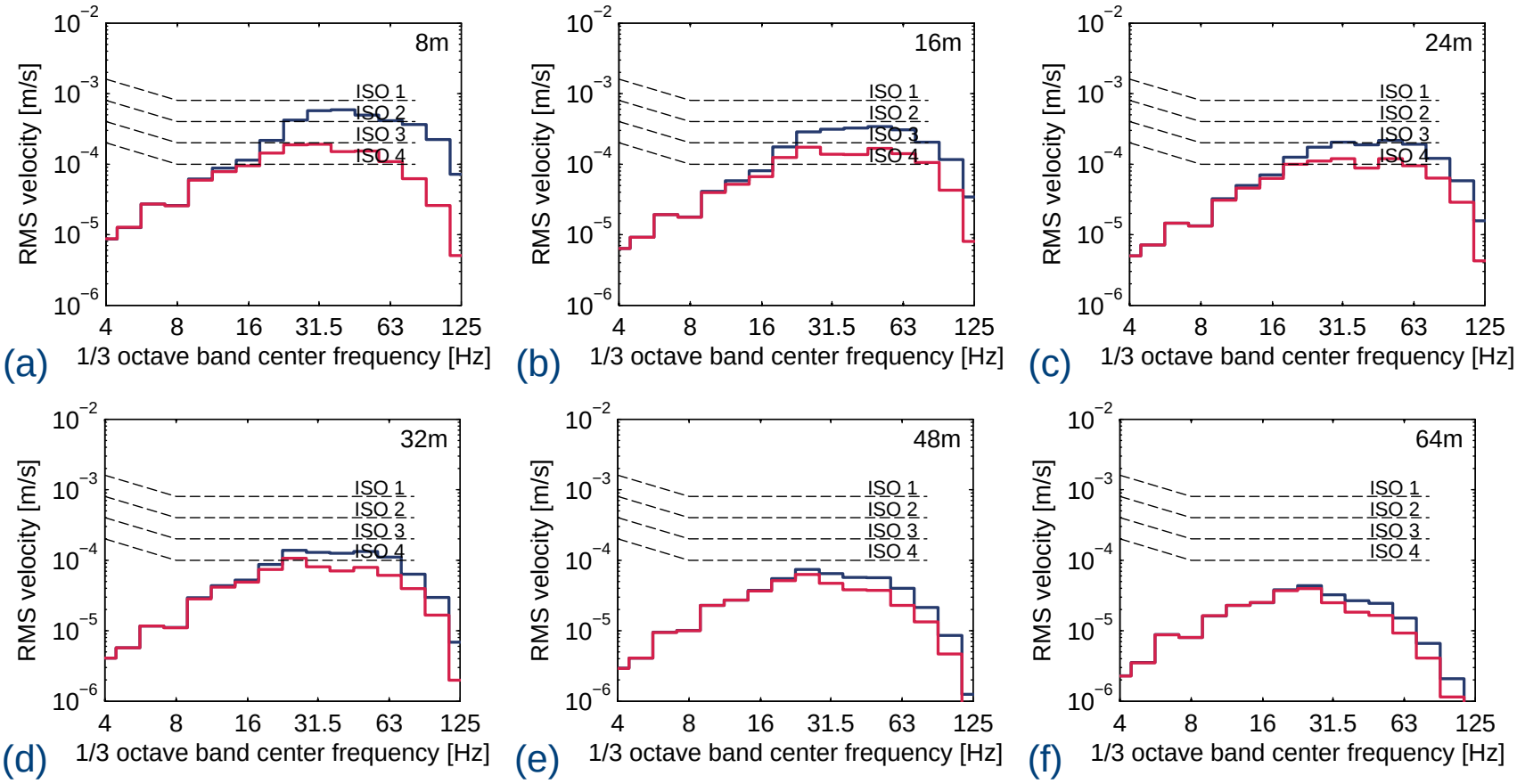

Experimental validation

- A continuous stiff wave barrier of $1\,\mathrm{m} \times 7.5\,\mathrm{m} \times 55\,\mathrm{m}$ has been installed in El Realengo (Spain) within the EU FP7 project RIVAS ("Railway Induced Vibration Abatement Solutions")

- Measured free field velocity at (a) $18\,\mathrm{m}$ and (b) $32\,\mathrm{m}$ from the track center at the *reference site* and at the *test site*. The barrier is situated at $16.2\,\mathrm{m}$ from the track center.

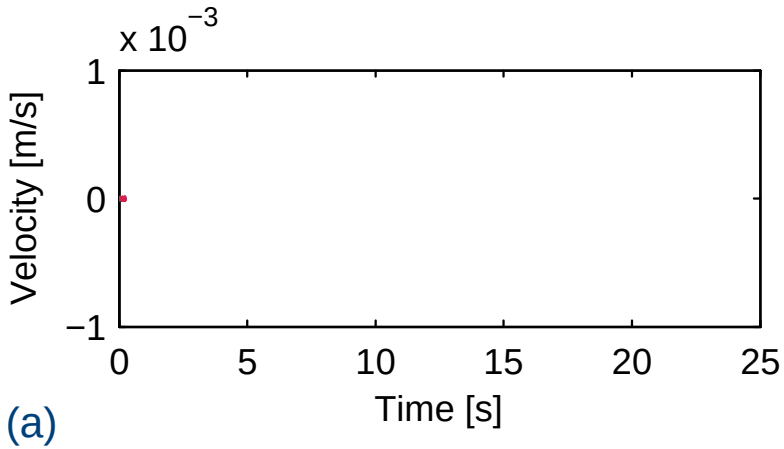

(a)

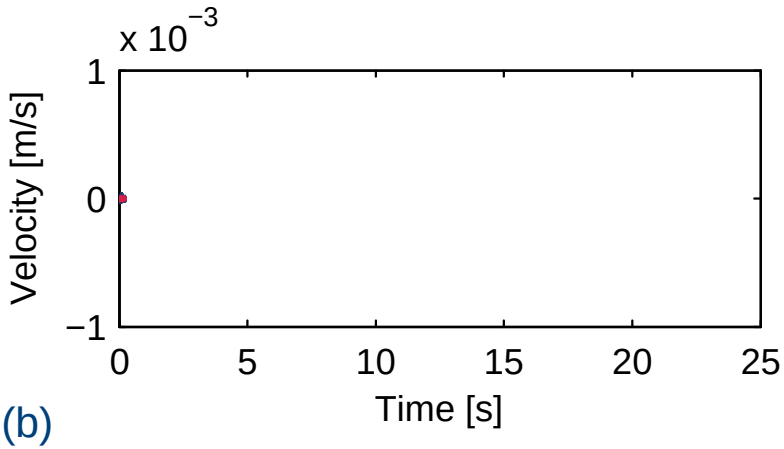

(b)

Experimental validation

- Measured vibration velocity level due the passage of RENFE S599 trains at an average speed of $118\,\mathrm{km/h}$ at the *reference site* and at the *test site* before (dashed line) and after (solid line) installation of the barrier, at (a) $10\,\mathrm{m}$, (b) $14\,\mathrm{m}$, (c) $18\,\mathrm{m}$, and (d) $32\,\mathrm{m}$ from the track center. The barrier is situated at $16.2\,\mathrm{m}$ from the track center.

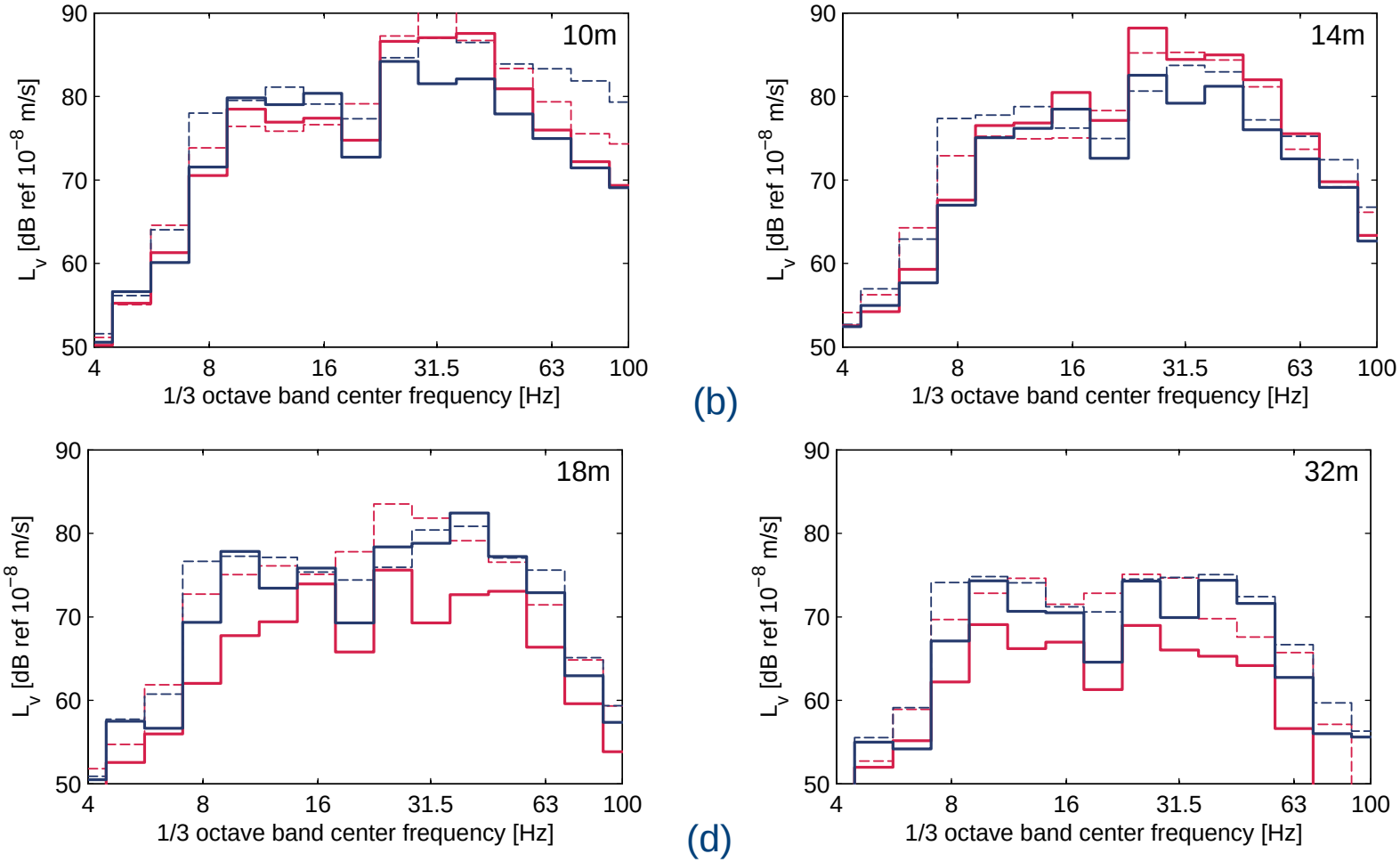

Experimental validation

- *Predicted* and *measured* vertical insertion loss for RENFE S599 trains at an average speed of $118\,\mathrm{km/h}$ at (a) $10\,\mathrm{m}$, (b) $14\,\mathrm{m}$, (c) $18\,\mathrm{m}$, and (d) $32\,\mathrm{m}$ from the track center. The barrier is situated at $16.2\,\mathrm{m}$ from the track center.

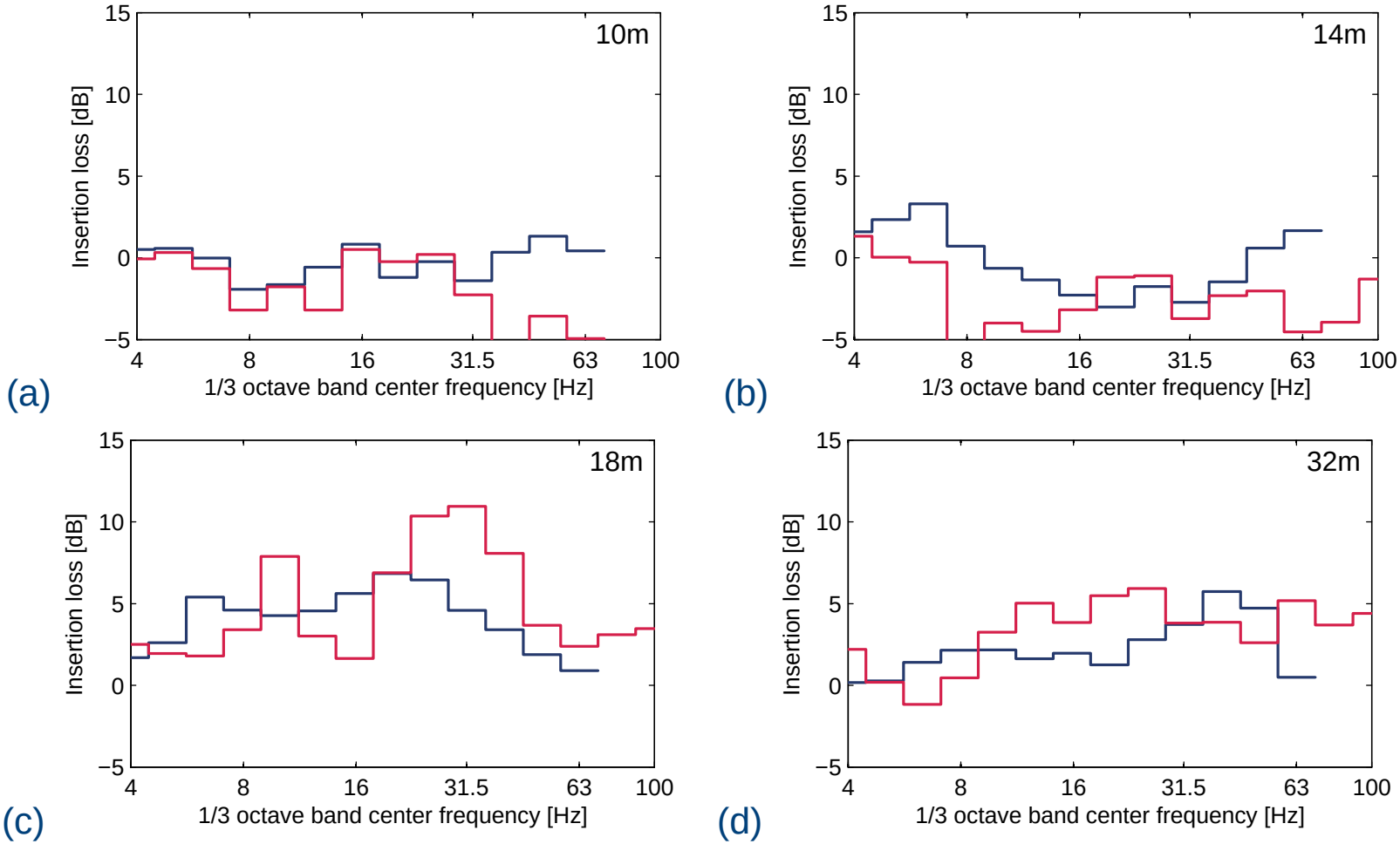

Wave propagation in an urban environment

- Urban environment (e.g. Tokyo): different buildings interact with each other due to interference of the scattered waves

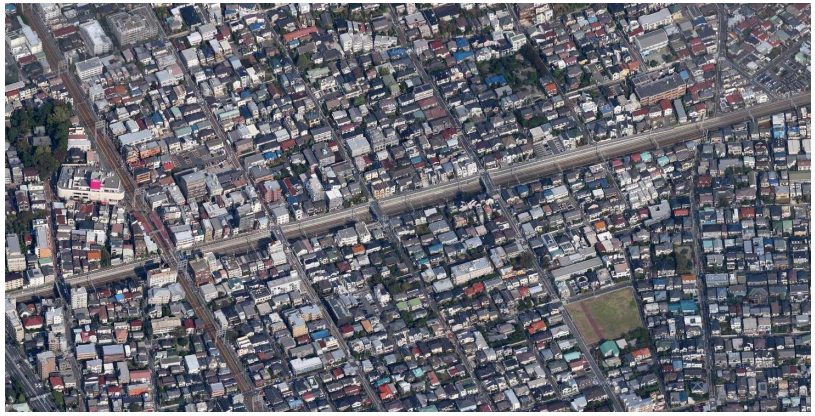

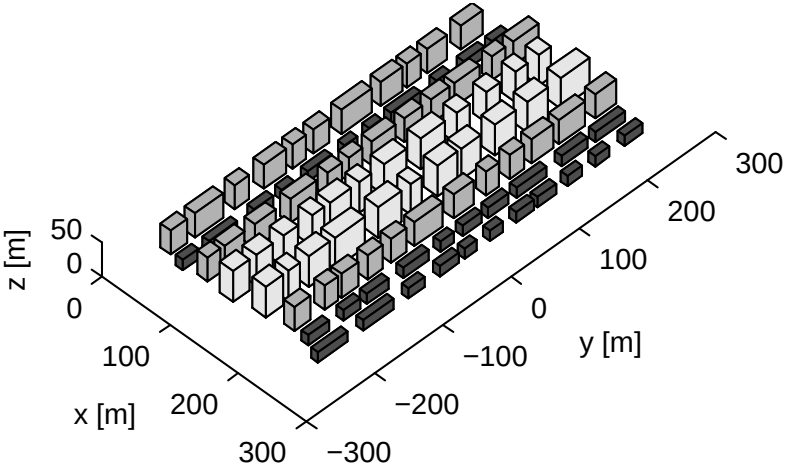

- The developed numerical techniques enable the simulation of wave propagation in an urban environment

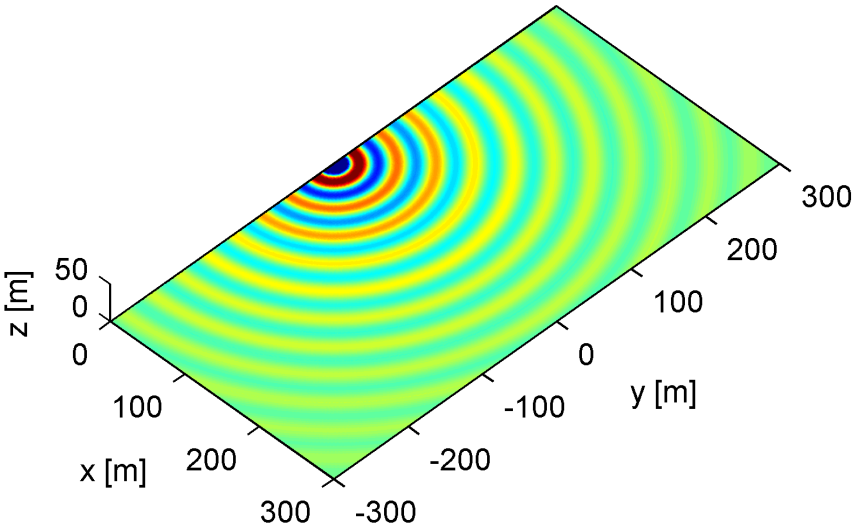

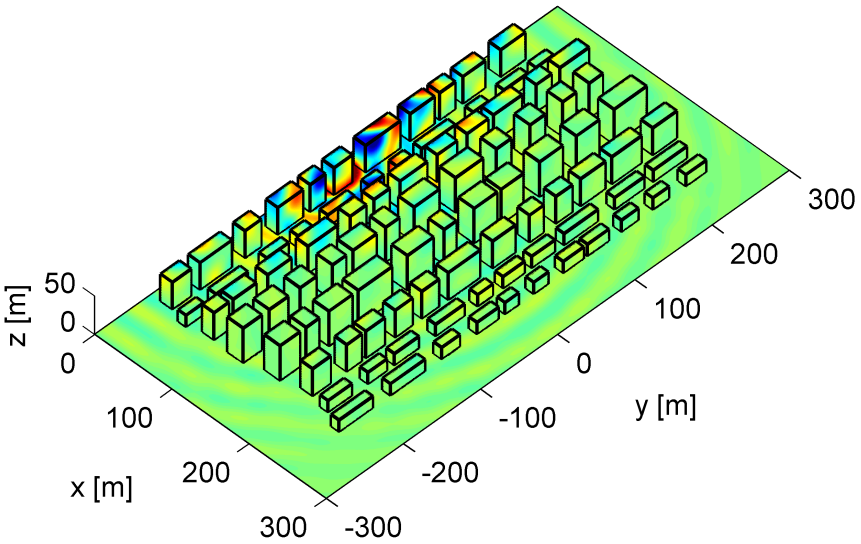

Wave propagation in an urban environment

- Urban environment (e.g. Tokyo): different buildings interact with each other due to interference of the scattered waves

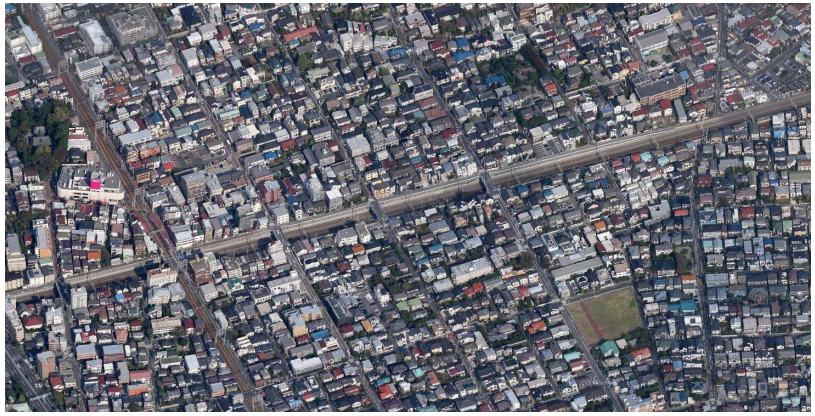

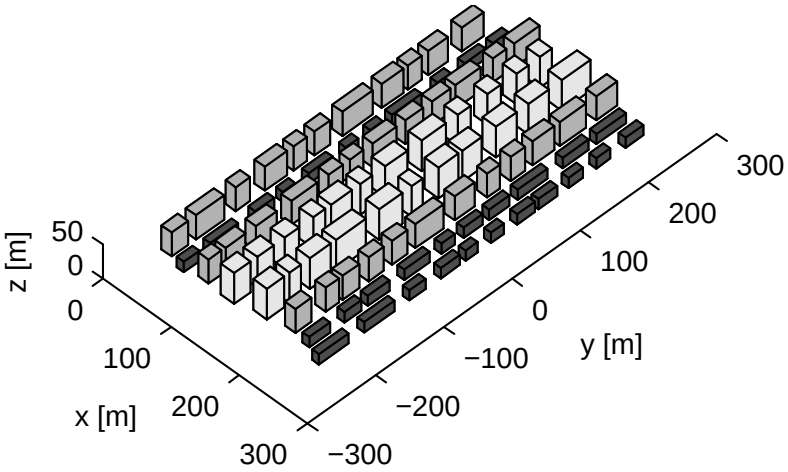

- The developed numerical techniques enable the simulation of wave propagation in an urban environment

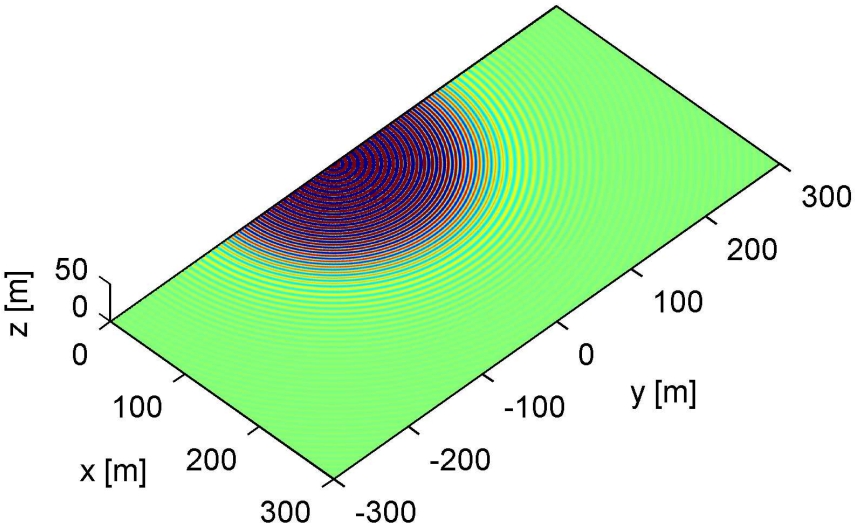

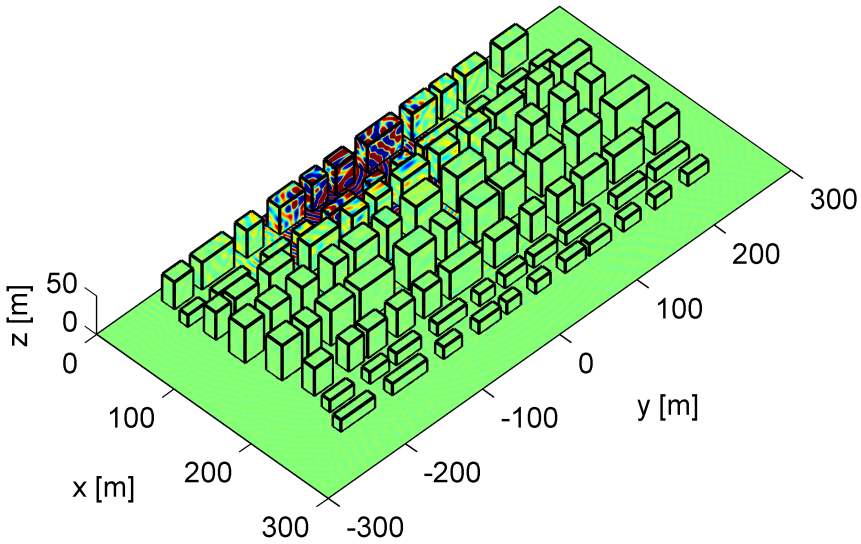

Conclusions

- Development of numerical techniques for dynamic SSI:
  - The application of $\mathscr{H}$–matrices along with appropriate FE–$\mathscr{H}$-BE coupling methodologies enables the evaluation of large 3D FE–BE models
  - Spatial windowing allows applying 2.5D models even if the assumption of longitudinal invariance is not fulfilled

- Railway induced vibrations:
  - A stiff wave barrier is an effective vibration countermeasure at a site with soft soil layers
  - Dynamic through–soil coupling of buildings affects the wave propagation in an urban environment

Recommendations for further research

- Development of numerical techniques for dynamic SSI:
  - non–conforming FE–BE interfaces
  - time domain FE–$\mathscr{H}$-BE models

- Railway induced vibrations:
  - efficient solution of inverse problems
  - efficient solution of optimization problems

- Other applications: earthquakes induced by the extraction of natural and shale gas, design of foundations for offshore wind turbines and oil platforms, . . .

KU LEUVEN

Wave Mechanics Seminar
TU Delft
May 19, 2014

The numerical solution of large scale dynamic soil–structure interaction problems

Pieter Coulier

pieter.coulier@bwk.kuleuven.be
bwk.kuleuven.be/bwm

KU Leuven, Department of Civil Engineering, Belgium